Extreme mobility creates contrasting patterns of panmixia, isolation-by-distance and hybridization in four flying-fox species (*Pteropus*)

Armin Scheben[1*], Adam McKeown[2], Tom Walsh[3], David A. Westcott[4], Suzanne S. Metcalfe[5], Eric P. Vanderduys[5] and Bruce L. Webber[6*]

[1] Simons Center for Quantitative Biology, Cold Spring Harbor Laboratory, Cold Spring Harbor, NY, 11724, United States of America
[2]CSIRO Environment, Adelaide, South Australia, 5052, Australia
[3]CSIRO Environment, Canberra, Australian Capital Territory, 2600, Australia
[4]CSIRO Environment, Atherton, Queensland, 4883, Australia; Present address: PO Box 1056, Atherton, Queensland, 4883, Australia
[5]CSIRO Environment, Brisbane, Queensland, 4102, Australia
[6]CSIRO Health and Biosecurity, Floreat, Western Australia 6014, Australia; School of Biological Sciences, University of Western Australia, Crawley, Western Australia 6009, Australia; Present Address: Bush Heritage Australia, 637 Flinders St, Docklands, Victoria 3008, Australia.

*To whom correspondence should be addressed: armin.scheben@gmail.com, bruce.webber@uwa.edu.au

Abstract

Speciation results from shifts between genetic connectivity and isolation of populations. Flying-foxes (*Pteropus*) are a compelling model to study the interplay of these evolutionary processes due to their rapid radiation in the island-rich region of the Indo-Australian Archipelago. Here, we investigate the population genetics of the highly mobile flying-foxes *Pteropus alecto*, *P. conspicillatus*, *P. poliocephalus*, and *P. scapulatus* across large parts of their overlapping ranges in Australia, Indonesia, and New Guinea. Using reduced-representation sequencing, we examined the extent to which panmixia, isolation-by-distance, and hybridization are prevalent in these populations. Phylogenetic and demographic modeling approaches indicate that isolation-by-distance, despite ongoing gene flow, occurs in *P. alecto* and *P. conspicillatus* populations while *P. poliocephalus* and *P. scapulatus* are panmictic across Australia. We further find that

hybridization and asymmetric gene flow from *P. conspicillatus* to *P. alecto* plays a role in shaping the historic and contemporary populations of these recently diverged species, which exhibit gene flow along a geographic ring connecting Indonesia to Australia and New Guinea. Together, our findings indicate that long-range population connectivity and limited restrictions on gene flow have shaped the evolution and diversification of flying-foxes.

1 Introduction

Dispersal influences the evolutionary trajectory of species, both promoting speciation through geographic isolation and counteracting it by maintaining genetic connectivity (Lomolino, 2000). Through its effect on gene flow, range expansions, and colonization ability, dispersal thus plays a complex role in allopatric speciation, though speciation may also occur in sympatry due to non-geographic barriers such as ecological divergence (Richards et al., 2019). Many species capable of long-distance dispersal form panmictic populations across continents (Bruxaux et al., 2024; Neethling et al., 2008; Peel et al., 2013; Reich et al., 2024; Reudink et al., 2011). In contrast, genetic isolation-by-distance is also widespread, leading to correlations between populations' geographic structure and their genetic structure (Aguillon et al., 2017; Sharbel et al., 2000; Wright, 1943). Panmixia and isolation-by-distance can occur within species at various spatiotemporal scales and incipient speciation can be prevented by secondary contact if populations are not sufficiently reproductively isolated. Alternatively, secondary contact can lead to reinforcement of species boundaries, and long-lasting natural hybrid zones can even be maintained despite gene flow across large geographic distances (Abbott et al., 2013). In rare cases, reproductively isolated populations connected by interbreeding populations around geographic barriers may form "ring species" (Irwin et al., 2005). Although ideal ring species may not exist, 'broken' ring species without continuous gene flow during divergence can still provide insights into ringlike evolutionary dynamics (Alcaide et al. 2014; Kuchta & Wake, 2016). However, our understanding of these complex stages of dispersal and speciation remains limited by how infrequently these processes have been investigated in recently diverged highly mobile species.

Bats are the only mammals capable of powered flight and make up the second-most species-rich mammal group with 1,487 species (Simmons & Cirranello, 2025). Flying-foxes (*Pteropus*;

Pteropodidae) are a particularly fast-radiating and recently diverged genus of bats originating in the Wallacea region of the Indo-Australian Archipelago (Tsang et al., 2020). The rapid diversification of flying-foxes has been associated with their high long-distance dispersal rate compared to other volant species (Tsang et al., 2020), enabling them to colonize new and isolated habitats such as archipelagos, where subsequent geographic isolation promotes allopatric speciation (Smyčka et al., 2023). Individual flying-foxes are capable of long-distance movements (Breed et al., 2010; Eby, 1991; Westcott et al., 2015), with tracking experiments showing some individuals covering over 100 km a day (Roberts et al., 2012) and an average of 1,427-6,073 km annually (Welbergen et al., 2020). Flying-fox biogeography reflects this extreme mobility, with repeated colonisations of remote oceanic islands (O'Brien et al., 2009). While all Australian flying-fox species are known to make long-distance movements, the extent and frequency of connectivity between different parts of species' ranges, how this is influenced by geography, and the evolutionary consequences are virtually unknown.

Four flying-fox species are native to the Australian mainland: the black flying-fox (*Pteropus alecto*), spectacled flying-fox (*P. conspicillatus*), grey-headed flying-fox (*P. poliocephalus*), and little-red flying-fox (*P. scapulatus*). While *P. poliocephalus* is endemic to Australia, the other species have disjunct distributions extending to Indonesia and New Guinea (Figure 1). An early genetic study found that the widespread Australian *P. alecto*, *P. poliocephalus*, and *P. scapulatus* were panmictic, suggesting these bats resembled migratory species (Webb & Tidemann, 1996). The less widely distributed *P. conspicillatus* has a notably smaller population size compared to the other species and is listed as endangered in Australia (Roberts et al., 2020). Previous work has hypothesized that hybridization occurs between Australian *P. alecto* and both *P. conspicillatus* (Fox, 2006; Neaves et al., 2018) and *P. poliocephalus* (Webb & Tidemann, 1995) based on limited genetic evidence. *P. alecto* and *P. conspicillatus* are morphologically highly similar, with the key distinguishing morphological feature of *P. conspicillatus* being its eye-rings, though light eye-rings also occur in *P. alecto* (Neaves et al., 2018). The phylogenetic relationship of these two species has been resolved inconsistently across a number of studies using small sets of nuclear and mitochondrial genes (Almeida et al., 2009; Almeida et al., 2014; Almeida, 2020; Fox, 2006; Tsang, 2015; Tsang et al., 2020). One phylogenetic study found that *P. alecto* nested within *P. conspicillatus*, explaining this through incomplete lineage sorting or hybridization (Almeida et al., 2009). Their divergence-time is variously estimated at 1-2 million

years ago (mya) (Tsang, 2015) or 2-3 mya (Tsang et al., 2020). Intriguingly, their geographic distribution across Australia, Indonesia, and New Guinea suggests that *P. alecto* and *P. conspicillatus* may represent a ring species.

In this work, we investigate the population genetic structure of *P. conspicillatus*, *P. alecto*, *P. poliocephalus*, and *P. scapulatus* using genome-wide SNPs. We aim to determine 1) how the genetic structure of these four flying-fox species differs across their distributions, 2) what role hybridization has played in their evolution, and 3) whether *P. alecto* and *P. conspicillatus* form a ring species. We hypothesize that mainland Australian flying-fox populations are panmictic, but that Indonesian populations of *P. alecto* and New Guinean populations of *P. conspicillatus* are genetically distinct from Australian populations. In addition, we hypothesize that *P. alecto* hybridizes with the related flying-fox species *P. conspicillatus* and *P. poliocephalus* in regions of overlapping distribution. Finally, we hypothesize that *P. alecto* and *P. conspicillatus* form an interbreeding population with gradual isolation-by-distance along the geographic ring connecting Australia with Indonesia, and New Guinea, with the endpoint in Central Indonesia.

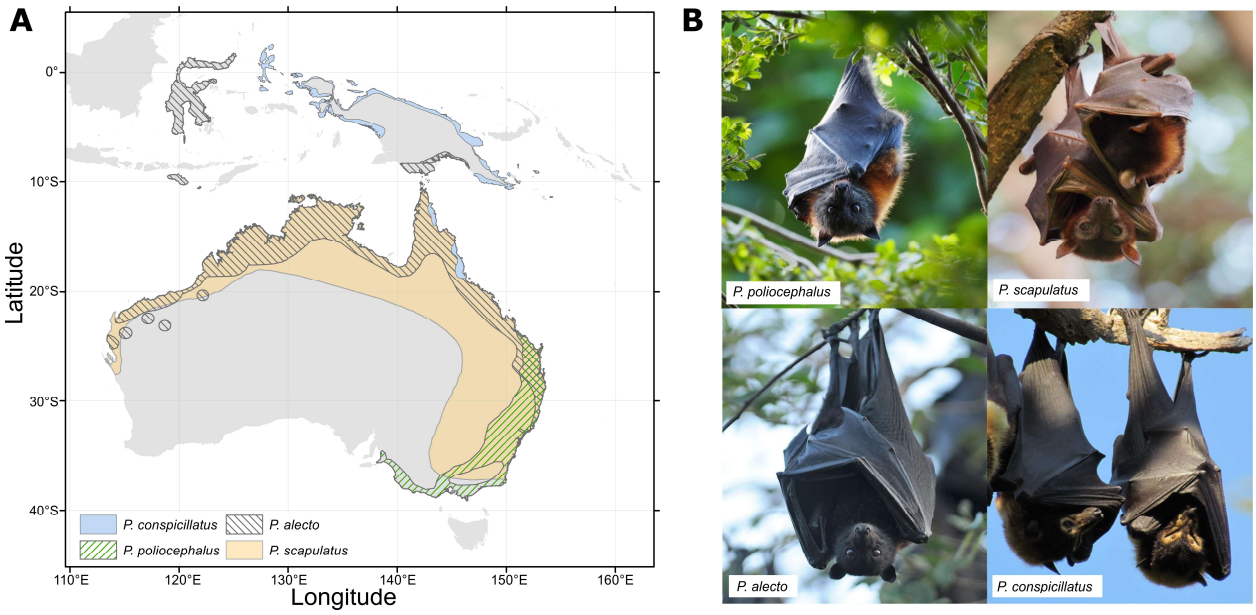

Figure 1. Sampled *Pteropus* flying-fox species and their geographic distributions. A) Ranges of the four flying-fox species native to the Australian mainland (https://www.iucnredlist.org). B) Photographs of the four flying-fox species. Image credit: Adam McKeown and Eric P. Vanderduys.

2 Materials and methods

2.1 Sample collection

Small 3mm circles of skin were removed from the wing membrane of individual flying-foxes using a biopsy punch. The animals were captured in accordance with animal ethics approval (Permit number CSIRO AEC 2016-17). Wing punches were obtained from individuals of the four different flying-fox species, *P. alecto*, *P. poliocephalus*, *P. scapulatus*, and *P. conspicillatus*. A total of 288 flying-fox samples were collected from 27 roost locations in Australia and New Guinea as well as 4 locations in Indonesia (Table S1). The samples included 33 historical *P. alecto* specimens collected between 1989 and 2003 from the Western Australian museum collection (WAM).

2.2 Genomic library preparation, sequencing, and variant calling

Genomic DNA was extracted using the Qiagen DNA Blood and Tissue Kit (Hilden, Germany). A total amount of 100 ng of genomic DNA from each individual was digested in a 50 µL reaction with 20 units each of high-fidelity restriction enzymes, PstI and EcoRI (New England Biolabs, Ipswich MA, USA) and a sequencing library prepared (see Text S1 for additional details). Sequencing was conducted using the 75bp PE v3 sequencing kit on an Illumia NextSeq. Reads were aligned to the *P. alecto* reference genome ASM32557v1 (Zhang et al., 2013) from GenBank using bwa mem 0.7.17-r1198-dirty (Li, 2013) with default settings. The low-quality 5bp flanking regions of all reads were trimmed. Using bcftools 1.19 (Danecek et al., 2021), a pileup was generated with a minimum base quality of 10 and minimum mapping quality of 20 and variants were called, applying Hardy-Weinberg equilibrium assumptions within populations using the -G flag. Invariant sites were included to inform demographic modelling. Following variant calling, pre-analysis quality control of alignment metrics, preliminary phylogenetic species assignment, and duplicate removal were conducted, excluding 46 samples (Text S2 and Table S1). Variant calling was then repeated using the final set of 242 samples.

The variant calls were split into three datasets for filtering and analysis (Table S2): an “all” set containing all four species (n=242), an “alecto + conspicillatus” set (n=150), and an “alecto ex alecto alecto + conspicillatus” set (n=141). Filtering was conducted separately for these datasets

136 to minimize the number of SNPs excluded due to missingness in species-specific analyses. Sites
137 were filtered using vcftools 0.1.16 (Danecek et al., 2011) using a minimum depth of 5, a
138 minimum genotype quality of 20, a minimum minor allele frequency of 0.05, and a maximum
139 missingness of 20% across all samples. Next, variants were filtered to retain only biallelic SNPs.
140 PLINK2 2.00a2.3LM (Chang et al., 2015) was used to prune linked SNPs with "--indep-pairwise
141 50 5 0.3". Kinship coefficients were calculated using the KING algorithm (Manichaikul et al.,
142 2010) as implemented in PLINK2.

143 2.3 Population genetic analysis

144 By investigating genetic diversity, relatedness, and admixture, we aimed to characterize the
145 genetic differentiation, connectivity, and potential hybridization among *Pteropus* species across
146 their geographic ranges. For this population genetic investigation, individuals were assigned to
147 six geographic regions: Indonesia, North West Australia, North East Australia, East Australia,
148 Wet Tropics Australia, and New Guinea (Figure S1). The Wet Tropics region of Queensland,
149 Australia is a unique region of wet tropical forests and distinct from other sampled locations in
150 North East Australia. To limit species-specific biases in the per-species heterozygosity and
151 nucleotide diversity estimates, we split the unfiltered "all" SNP set with invariant sites by species
152 and then filtered for minimum depth of 5, minimum genotype quality of 20, and maximum
153 missingness of 20%. We then assessed nucleotide diversity including multiallelic sites in non-
154 overlapping 100kb windows using pixy 1.2.11.beta1 (Korunes & Samuk, 2021), removing
155 windows with fewer than 50 sites. We calculated heterozygosity per sample using bcftools
156 including multiallelic sites. Using the "all" and the "alecto + conspicillatus" SNP sets, we next
157 calculated genome-wide genetic differentiation (F_{ST}) for population pairs using stacks
158 populations 2.52 (Rochette et al., 2019). To elucidate genetic structure, a principal component
159 analysis (PCA) was carried out on these SNPs with SNPRelate 1.40.0 (Zheng et al., 2012). Using
160 the same data, we next inferred phylogenetic trees using RAxML 8.2.12 (Stamatakis, 2014) with
161 the GTRCAT model to account for using only variant sites and 100 bootstraps. Because the
162 assumption of all sites sharing a genealogical history may not hold, we also inferred phylogenies
163 with the coalescent approach CASTER-site 1.23.2.6 (Zhang et al., 2025). To investigate
164 between-species divergence-times, we used SNAPP (Text S3).

For all further analyses we focused on *P. alecto* and *P. conspicillatus*, relying on the "alecto + conspicillatus" SNP set or, where *P. alecto alecto* was not included, the "alecto ex alecto alecto + conspicillatus" SNP set. To detect admixture and potential hybridization, population structure was inferred using fastSTRUCTURE 1.0 (Raj et al., 2014) with 1 to 15 clusters and the default prior, using the provided chooseK method to select an optimal number of clusters that maximizes the log-marginal likelihood lower bound of the data. Admixture proportions for individuals were estimated as continuous values representing membership fractions across clusters, with no fixed threshold for cluster assignment, and clusters were interpreted qualitatively by linking them to species and geographic regions. To validate potential hybridization inferred using admixture analysis, we selected ancestry-informative markers with a species-specific allele frequency of at least 0.85 and used them to generate triangle plots of hybrid index and interclass heterozygosity using triangulaR (Wiens & Colella, 2024). Individuals with over one third of ancestry-informative markers missing were excluded from the analysis.

2.4 Gene flow inference

To elucidate the extent and direction of historical and contemporary gene flow between geographic populations of *Pteropus alecto* and *P. conspicillatus*, we used a set of complementary population genetic analyses. Migrations between the six geographic populations of *P. alecto* and *P. conspicillatus* were firstly inferred using Treemix 1.13 (Pickrell & Pritchard, 2012) with the Indonesian *P. alecto alecto* individuals set as the outgroup. Treemix uses SNP-based allele frequency data to infer discrete migration events, which are modelled as migration edges m between populations on a phylogenetic tree. We ran Treemix with 500 SNPs per block for covariance matrix estimation and values of m ranging from 0-7, with 10 replicates for each value. We then used the Evanno method implemented in the R package OptM to determine the optimal value of m (Fitak, 2021). We next computed an additional 100 replicates using the optimal value of m and selected the replicate with the highest likelihood. To complement the Treemix analysis by also explicitly exploring spatial genetic structure, we applied FEEMSmix 2.0.0 to calculate an effective migration surface (Shastry et al., 2025). FEEMSmix adds long-range migration to the FEEMS framework, which infers migration rates on the edges of a graph of connected nodes representing local populations. Cross-validation was used to identify the tuning parameters comprising the migration edge weight penalty (λ=0.05) and the node-specific

variance penalty (λ_q=100). These tuning parameters penalize the strength of migration by homogenizing neighboring nodes and edges.To better model continuous gene flow across different time periods, we next investigated gene flow between and within the *P. alecto* and *P. conspicillatus* populations using coalescent simulations based on the site frequency spectrum implemented in fastsimcoal2 2.8 (Excoffier et al., 2013). To avoid overlap between populations, three specimens from North West Australia (M53754, M54659, M54660) from the Indonesian fastSTRUCTURE cluster were excluded from this analysis. To account for missing data, we maximized the number of segregating sites by using a projection of samples based on EasySFS (https://github.com/isaacovercast/easySFS) which relies on methods implemented in dadi (Gutenkunst et al., 2009). The "--total-length" parameter was set based on the variant and the invariant sites detected in the aligned reads for each population pair. We defined four demographic scenarios for comparison between population pairs: strict isolation, ancient migration, recent migration, and constant migration (Figure 2). We allowed for asymmetric migration between populations. We assumed a mutation rate of 2.5×10^{-8} mutations per nucleotide site per generation (Nachman & Crowell, 2000; Sovic et al., 2016) and a generation time of 4 years (McIlwee & Martin, 2014). To evaluate the demographic scenarios, we ran fastsimcoal2 for 100 replicates per migration scenario using the parameters "-m -n 50000 -L 30 -M -C 10". After selecting the replicate with the highest maximum composite likelihood for each scenario, we used the Akike information criterion (AIC) to determine the best fitting migration scenario for each population pair, assessing consistency with the corrected AIC (cAIC). Next, to calculate confidence intervals for all model parameter estimates, we ran 100 parametric bootstrap replicates by simulating site frequency spectra from the estimates of each of the best-fitting models (Excoffier et al., 2013).

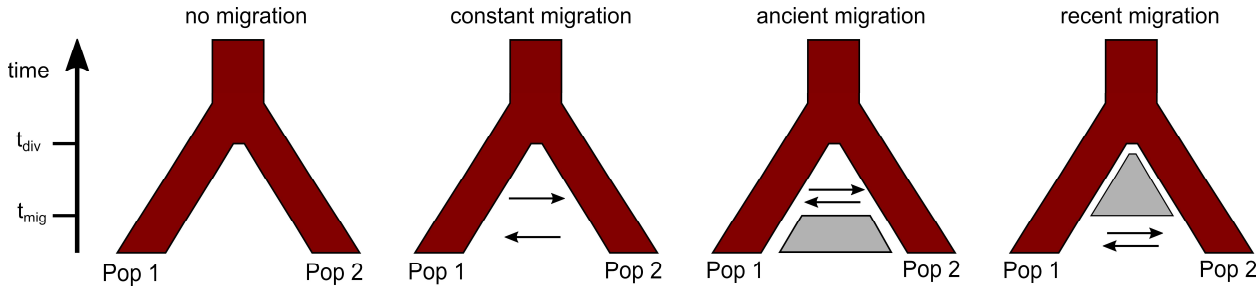

Figure 2. Migration models for pairwise demographic histories between populations. Each model includes a parameter for the time that populations split (t_{div}) and models with non-constant migration

221 include a parameter for the time that migration began or ceased (t_{mig}) depending on whether the migration
222 occurred recently or in the past. Grey boxes indicate barriers to gene flow.

223 3 Results

224 3.1 Sequencing, read processing, quality control, and variant calling

225 A total of 242 of 288 samples were retained following quality control (Table S1). For each
226 sample passing quality control, an average of 2.14m read pairs (SD = 0.79m) of 43bp trimmed
227 length were generated. The average alignment rate to the *P. alecto* reference genome was
228 95.12% (SD=1.45%), covering an average of 4.39% (SD=1.62%) of the genome and 7.95%
229 (SD=3.11%) of the coding regions with an average 1.8-fold (SD=0.13) overrepresentation of
230 coding regions (Table S1). The average per species percentage of covered regions that were
231 coding took on a narrow range of 6.56-7.51%. Alignment rates did not differ between *P. alecto*
232 and *P. conspicillatus* (mean=96.2%, unpaired *t*-test Holm-adjusted p=1) but alignment rates for
233 the more diverged species *P. poliocephalus* (mean=93.1%, unpaired *t*-test Holm-adjusted
234 $p=1.59\times10^{-50}$) and *P. scapulatus* (mean=94.3%, unpaired *t*-test Holm-adjusted $p=6.26\times10^{-24}$)
235 were slightly lower. A total of 1,339,950 raw variants were detected and then filtered for
236 minimum allele depth, missingness per variant, minor allele frequency, and linkage
237 disequilibrium (see Methods). For the "all" dataset, 11,818 filtered SNPs with an average per-
238 sample depth of 17.90× were retained after filtering. For the "alecto + conspicillatus" dataset,
239 17,708 SNPs with an average per-sample depth of 16.83× were retained after filtering (Table
240 S2). The samples from the WA museum did not show significantly different genotype
241 missingness rates compared to the extant samples (mean=13.4%, unpaired *t*-test p=0.20).

242 3.2 Population structure of four flying-fox species

243 We found a wide range of genome-wide diversity in the flying-fox species as measured by
244 heterozygosity H (Figure S2) and nucleotide diversity π (Figure S3). Based on the genetic
245 evidence, we split *P. alecto* into two groups for all analyses: the Indonesian taxon *P. alecto*
246 *alecto* (n=9) and all other *P. alecto* individuals (n=86). We found intermediate diversity relative
247 to the other species in *P. alecto* (mean H = 0.004, mean π = 0.004) and *P. conspicillatus* (mean

H = 0.003, mean π = 0.003). *P. scapulatus* had the highest diversity (mean H = 0.006, mean π = 0.005) and *P. poliocephalus* the lowest (mean H = 0.003, mean π = 0.002). *P. alecto alecto* was an outlier with a uniformly low diversity across samples (mean H = 0.003, mean π = 0.002). Across the four flying-fox species, we observed a wide range of between-species genetic differentiation, with F_{ST} ranging from 0.06 for *P. alecto* - *P. conspicillatus* to 0.33 for *P. scapulatus* - *P. alecto alecto* (Figure S4, Table S3). Within the closely related *P. alecto* - *P. conspicillatus* group (Figure S5, Table S4), F_{ST} values indicated low genetic differentiation between the New Guinean and the Australian *P. conspicillatus* (F_{ST}=0.01) but higher differentiation between the Indonesian and Australian *P. alecto* populations (F_{ST}=0.05-0.06). Additionally, we found that the Indonesian *P. alecto* population was most differentiated from the New Guinean *P. conspicillatus* (F_{ST}=0.14) and less differentiated from the Australian *P. conspicillatus* (F_{ST}=0.11).

PCA delineated the samples by species, but suggested close genetic association between *P. alecto* and *P. conspicillatus* (Figure 3, Table S5). Although *P. conspicillatus* showed limited population structure, *P. alecto* individuals formed mostly discrete groups by country as well as showing some separation within Australia between North West Australia and the remaining groups in East Australia and North East Australia (Figure 3D, Table S6). Based on population structure inference, the majority of Australian *P. alecto* individuals show signals of admixture, either from the Indonesian *P. alecto* cluster or from the *P. conspicillatus* cluster (Figure 3E). *P. alecto* individuals such as 1702005 and also *P. conspicillatus* individuals such as 1306014 show substantial admixture (Table S7). With an admixture proportion of 47.7% from the *P. alecto* cluster, the *P. conspicillatus* sample 1306014 is likely a hybrid or backcross. Missingness can spuriously pull samples to the center in PCA (Yi & Latch, 2022), but the missingness of 10.0% in this sample is average for the population (mean=10.0%, SD=9.5%). Furthermore, we did not find an effect of more relaxed genotype missingness thresholds on the PCA results (Figures S6 and S7). We also confirmed that the clustering of Indonesian and North West Australian samples from the WA museum was not related to biases in genotype missingness by conducting an additional PCA excluding all SNPs with missing genotypes (Figure S7). An evaluation of the effect of genotype missingness thresholds on the admixture analysis also found high consistency (Pearson's correlation > 0.99) in per-sample admixture proportions between a filter of up to 20% missingness and filters of up to 50%, 40%, and 30% (Table S7).

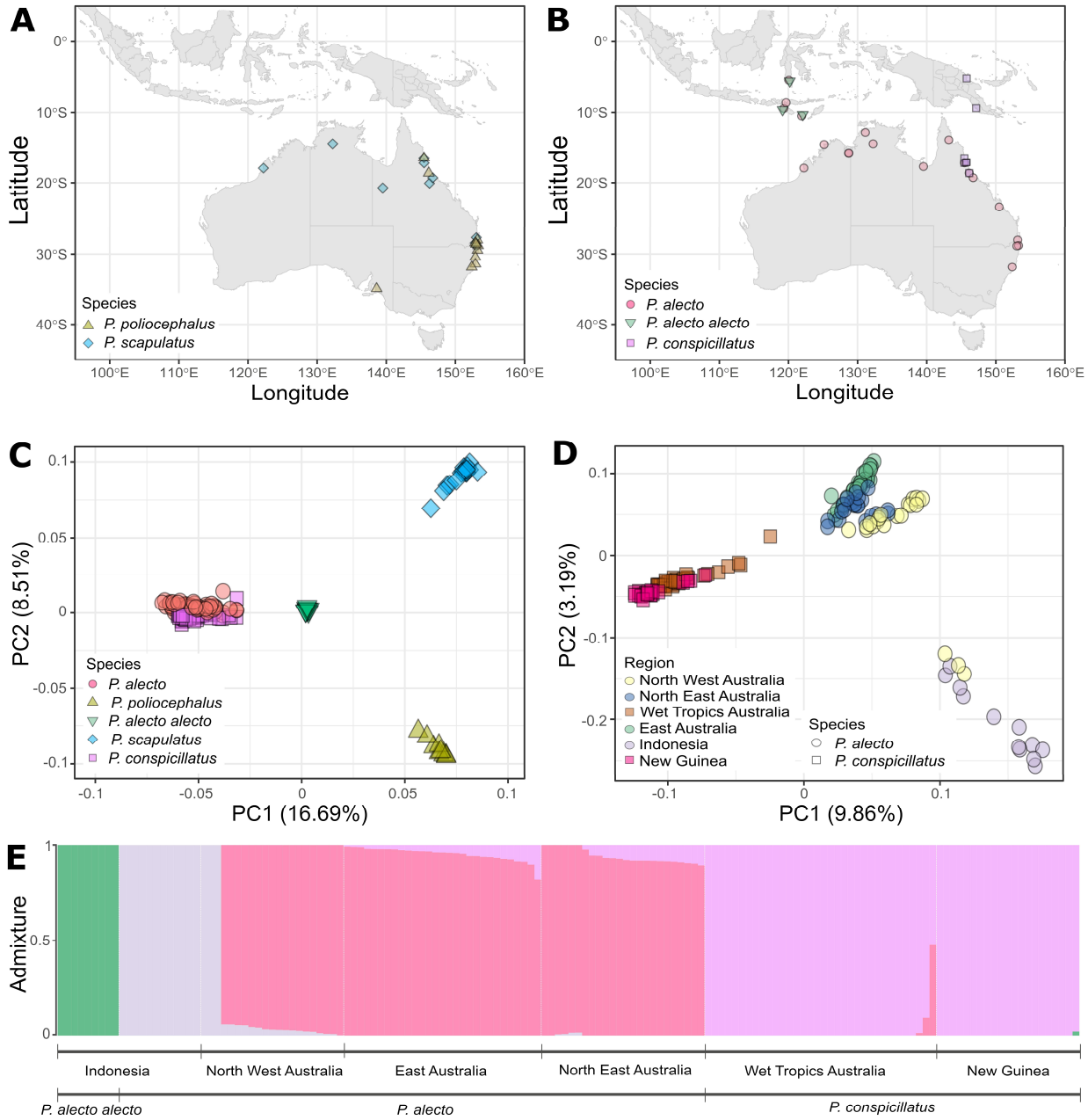

Figure 3. Population structure of four flying-fox species in Australia, Indonesia, and New Guinea. A) Sampling locations for *Pteropus poliocephalus* and *P. scapulatus*. B) Sampling locations for *P. alecto* and *P. conspicillatus*. C) SNP-based principal component analysis (PCA) of all sampled species. The percentage of genetic variance explained by each PC is shown on the axis. D) SNP-based PCA of six geographic populations of *P. alecto* and *P. conspicillatus*. The individual intermediate between the *P. conspicillatus* and the main Australian *P. alecto* cluster is sample 1306014. E) Structure plot of *P. alecto* and *P. conspicillatus* samples with four admixture groups. Bars indicate the proportion of each sample assigned to each group, revealing admixture between groups.

PCA and model-based population structure inference cannot readily distinguish admixture from isolation-by-distance and may thus not be sufficient to infer hybridization (Wiens & Colella, 2025). We therefore calculated hybrid indices of all *P. alecto* and *P. conspicillatus* individuals, representing the proportion of ancestry received from each parental population based on a set of 15 ancestry-informative markers. The triangle plot based on hybrid index and interclass heterozygosity confirmed hybridization between the species, indicating that individual 1306014 is a *P. alecto* × F_1 cross (Figures S8 and S9). In addition, *P. alecto* individuals including 1610001, 1702007, and 1702026 as well as *P. conspicillatus* individual 37721 were identified as later backcross generations. Overall, signatures of admixture from the *P. conspicillatus* cluster to the *P. alecto* cluster are more prevalent, with the majority of *P. conspicillatus* individuals not showing evidence of admixture or hybridization.

A SNP-based maximum likelihood phylogeny of *P. alecto* and *P. conspicillatus* recovered robust (bootstrap support>70) clades grouping these two species as distinct from the outgroup, but none of the six geographic groups except Indonesia formed robust clades (Figure S10). The Indonesian *P. alecto* clade consisting of historical samples clusters with three historical individuals (M54660, M53754, and M54659) and an extant individual (1702031) sampled from North West Australia with robust bootstrap support. In contrast to *P. alecto* and *P. conspicillatus*, *P. poliocephalus* and *P. scapulatus* showed no geographic structure across the sampled populations (Figure S11). Although the genealogical history of the samples may violate some of the assumptions of the maximum likelihood phylogeny, the coalescent phylogenies were consistent with the maximum likelihood phylogenies (Figures S12 and S13).

3.3 Admixture occurs between *P. alecto* and *P. conspicillatus* populations along a geographic ring

We next investigated population splits and admixture events in more depth using a maximum likelihood approach to infer migration edges in a population tree and coalescent simulations based on the site frequency spectrum to infer migration rates. We found support for three migration edges connecting *P. conspicillatus* to *P. alecto* (Figure S14A). Within *P. alecto*, we found a migration edge supporting gene flow from Indonesia to North West Australia. The inferred effective migration surface emphasized high-levels of within-species connectivity,

317 including one weakly supported long-range migrations from East Australia to North West
318 Australia and one from Indonesia to Australia (Figure 4B).

319 To further probe patterns of gene flow between distant populations, we used coalescent
320 simulations to test multiple demographic scenarios including isolation and migration at three
321 different time scales. These coalescent simulations indicated recent migration after a period of
322 isolation and divergence between *P. conspicillatus* populations and all *P. alecto* populations,
323 forming a ring connecting Indonesia, Australia, and New Guinea (Table 1 and Figure S14B).
324 Migration between Indonesian and Australian *P. alecto* populations was estimated to have
325 ceased 245 ya, though based on cAIC model selection constant migration between Indonesian
326 and North West Australian is supported (Tables S8 and S9). Such migration in recent history is
327 consistent with the evidence of migration between Indonesia and North West Australia from the
328 historical *P. alecto* individuals collected from 1989 to 2003 (Figures 4A and S10).

329 Although we inferred migration connecting the chain of four *P. alecto* populations from
330 Indonesia to East Australia, we also found that genetic distance increased with distance in this
331 species (Figures 4C and 4D, Table S10). When investigating pairwise comparisons of genetic
332 and geographic distance for all *P. alecto* individuals (Figure 4D), we found a significant positive
333 correlation (Mantel test, r=0.26, p=0.001). Consistent with our population structure analyses,
334 fastsimcoal2 estimates also showed consistently higher migration from *P. conspicillatus*
335 populations to *P. alecto* populations. Divergence-times between *P. conspicillatus* and *P. alecto*
336 were estimated by fastsimcoal2 using a fixed mammalian mutation rate to be between 136,305
337 thousand years ago (kya) to 159,120 kya (Table S9). Bayesian species-level divergence-time
338 inference using a calibration point from an earlier dated phylogeny suggested that *P. alecto* and
339 *P. conspicillatus* diverged 322.4-1023.7 kya (Figure S15).

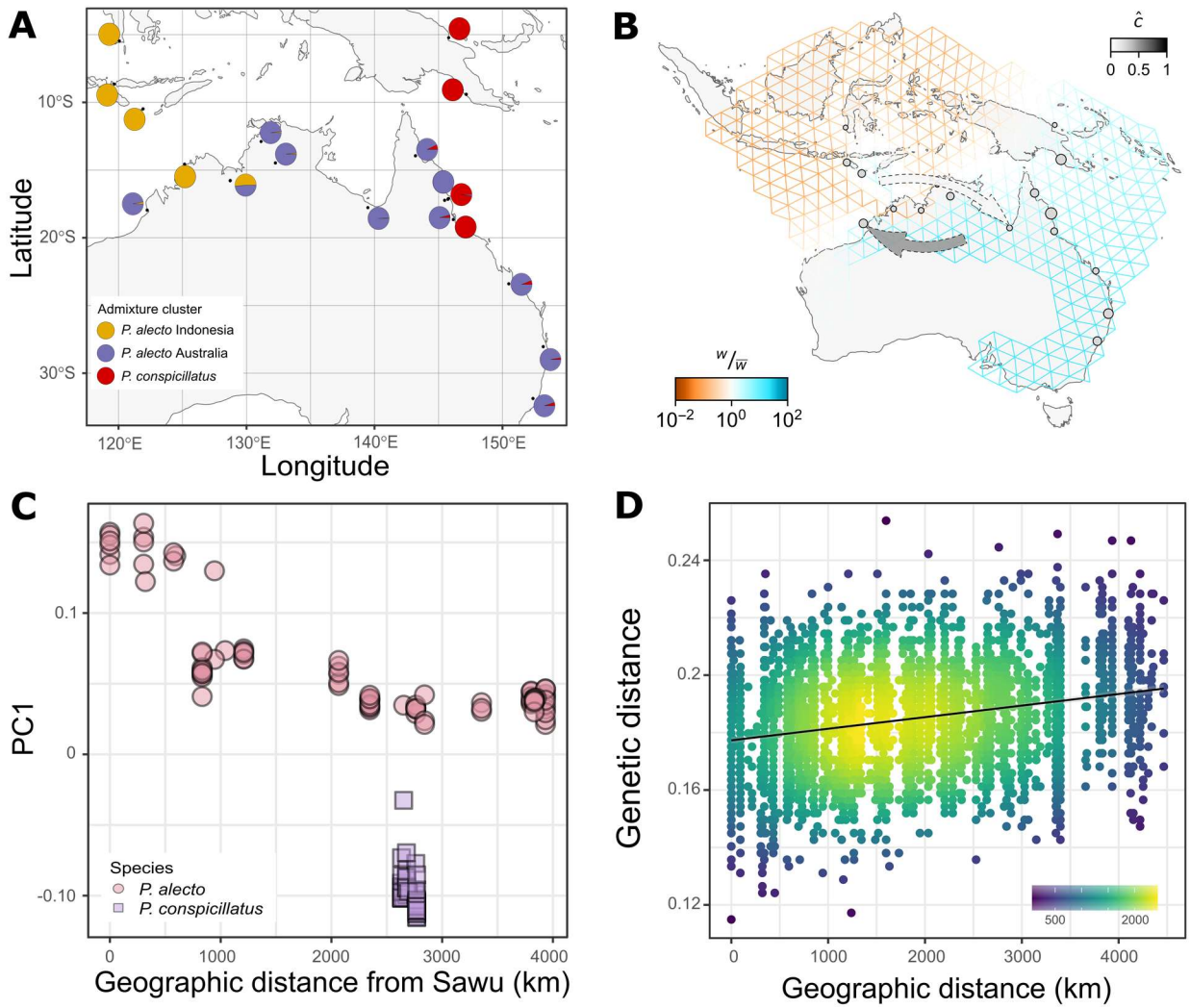

Figure 4. Gene flow in *Pteropus. alecto* and *P. conspicillatus* along a geographic ring ranging across Indonesia, Australia, and New Guinea. A) Admixture proportions for local demes of *P. alecto* and *P. conspicillatus*. Admixture is inferred via fastSTRUCTURE (see Figure 2E). B) Effective migration surface with long-range gene flow across the sampled distribution of *P. alecto* and *P. conspicillatus*. Weights (w) on the edges that represent migration rates between pairs of demes are shown relative to their mean value ($\underline{w}$) across all edges (Marcus et al., 2021). High migration regions are shown in blue and low migration regions in orange. Weakly supported long-range migration edges are indicated by dashed arrows, which are colored by the estimated source fraction ($\hat{c}$) (Shastry et al., 2025). C) Genetic differentiation is correlated with geographic distance in *P. alecto*. The first principal component (Table S6) is plotted against the geographic distance of each sample from Sawu, Indonesia, which is at one of the edges of the ring. D) Pairwise genetic distance in *P. alecto* is positively correlated with geographic distance. Each dot represents one non-redundant pair of the 86 sampled *P. alecto* individuals. Distance reflects the number of allelic differences between two individuals as a ratio of the observed and the possible differences.

356 **Table 1.** Inferred demographic parameters for four populations of *P. alecto* (Indonesia, North West Australia, North East Australia, and East
357 Australia) and two of *P. conspicillatus* (New Guinea and Wet Tropics Australia) based on coalescent simulation. The best of four migration
358 scenarios (isolation, ancient migration, recent migration, and constant migration) was selected based on the Akike information criterion. Years
359 since migration began are shown for recent migration and years since migration ended are shown for ancient migration. Estimates shown were
360 selected from 100 replicates based on the likelihood. For additional inferred demographic parameters and 95% confidence intervals see Table S9.

Pop 1	Pop 2	Best migration scenario	Migration from Pop 2 to Pop 1	Migration from Pop 1 to Pop 2	Years since migration began/ended
New Guinea	Indonesia	recent	5.71×10^{-6}	1.09×10^{-5}	59,971
New Guinea	North West Australia	recent	1.53×10^{-5}	2.93×10^{-5}	44,282
New Guinea	North East Australia	recent	1.88×10^{-5}	5.31×10^{-4}	31,726
New Guinea	East Australia	recent	1.42×10^{-5}	4.37×10^{-5}	51,045
New Guinea	Wet Tropics Australia	constant	9.37×10^{-5}	3.56×10^{-4}	NA
Indonesia	North West Australia	ancient	6.34×10^{-5}	2.88×10^{-5}	245
Indonesia	North East Australia	ancient	5.75×10^{-5}	2.22×10^{-5}	70,991
Indonesia	East Australia	ancient	3.72×10^{-5}	1.99×10^{-5}	851
Indonesia	Wet Tropics Australia	recent	1.48×10^{-5}	6.64×10^{-6}	47,224
North West Australia	North East Australia	constant	1.29×10^{-4}	2.26×10^{-4}	NA
North West Australia	East Australia	constant	1.96×10^{-4}	1.44×10^{-4}	NA
North West Australia	Wet Tropics Australia	recent	5.77×10^{-5}	4.39×10^{-5}	17,534
North East Australia	East Australia	constant	2.35×10^{-4}	1.41×10^{-4}	NA
North East Australia	Wet Tropics Australia	recent	8.48×10^{-5}	3.99×10^{-5}	21,570
East Australia	Wet Tropics Australia	recent	5.72×10^{-5}	2.81×10^{-5}	35,390

361

4 Discussion

Our investigation of genome-wide SNPs across 242 flying-fox individuals from four species revealed panmictic weakly differentiated Australian populations and strong isolation-by-distance in Indonesian *P. alecto* populations but not New Guinean *P. conspicillatus* populations. Both *P. poliocephalus* and *P. scapulatus* show no evidence of population structure within Australia, consistent with their large populations (Macdonald et al., 2021; Vanderduys et al., 2024), higher mobility relative to *P. alecto* (Welbergen et al., 2020), and limited geographic barriers in their eastern Australian range. Interestingly, we found that the Indonesian *P. alecto alecto* taxon (Andersen, 1912) forms a distinct lineage to the other *P. alecto* samples, diverging from *P. alecto* and *P. conspicillatus* ca. 2.61 mya. We expected higher genetic differentiation between disjunct *P. conspicillatus* populations, instead finding limited evidence for isolation between these populations based on summary statistics and coalescent modelling, suggesting that the roughly 150 km separating Australia and New Guinea does not represent a substantial geographic barrier for *P. conspicillatus*. Other flying-fox species including *P. vampyrus* and *P. niger* have also been shown to have limited population genetic structure and high connectivity between populations (Larsen et al., 2014; Tsang et al., 2018), though species such as *P. dasymallus* are known to exhibit isolation-by-distance between island populations (Chen et al., 2021).

High levels of population connectivity across their ranges helps explain the high genome-wide heterozygosity, an important measure of genetic diversity, which we found in all four species. Indeed, *P. alecto* is known to harbor higher heterozygosity than other mammals (He et al., 2023; Zhang et al., 2013). In our study, the use of a single *P. alecto* reference genome for all species even increased the potential for underestimation of genetic diversity and divergence in the more diverged *P. scapulatus* and *P. poliocephalus*, though the modest decrease in alignment rates of 2-3% for these species should only have a limited effect on our diversity estimates. A minor decrease in estimated diversity across species may also result from 6.5-7.5% of per-species genome coverage targeting coding regions rather than the 3.8% expected under fully unbiased sampling, which likely reflects overrepresentation of GC-rich coding regions that can arise in ddRAD sequencing due to biases in enzymes and DNA fragment size selection (DaCosta and

Sorenson, 2014). Despite this potential underestimation of heterozygosity, when compared to genome-wide heterozygosity in a diverse set of mammals ranging from 0.012% in domestic cat to 0.16% in gorilla (Cho et al., 2013), our findings of heterozygosity of 0.37% in *P. alecto* and 0.56% in *P. scapulatus* suggest that flying-foxes may generally be outliers with higher genetic diversity than other mammals.

Overall, we found that the higher degree of genetic diversity in Australian flying-fox populations compared with other populations is not primarily a result of admixture with sympatric species, as has been suggested (Tsang, 2015), but of strong within-species gene flow across Australia. Nevertheless, we found evidence of moderate hybridization between *P. alecto* and *P. conspicillatus* (Almeida et al., 2009). Consistent with hybridization rather than incomplete lineage sorting, admixed individuals primarily occurred in the broad region of distribution overlap in eastern Australia. However, hybrid backcross *P. alecto* individuals were not restricted to the narrow secondary contact zone with *P. conspicillatus* in the Wet Tropics region of Queensland, Australia. Instead, consistent with the high mobility of flying-foxes, hybrid backcrosses were widely distributed across eastern and northern Australia. We did not find any F_1 hybrids and only one F_2 hybrid and the modest number of substantially admixed individuals detected suggests that hybridization is ongoing but infrequent.

Field observations indicate that the morphologically highly similar *P. alecto* and *P. conspicillatus* inhabit ecologically distinct niches, with *P. alecto* found in savanna woodland and rainforest (Palmer et al., 2000) and *P. conspicillatus* primarily in rainforest (Richards, 1990). Although *P. conspicillatus* is not a true rainforest specialist (Parsons et al., 2007), this general divergence in ecological specialization may contribute to limiting gene flow between both species. These ecological niches may also have played a role in the initial divergence of these two species since niche conservatism can isolate diverging populations in distinct ranges during early allopatric speciation, but does not prevent secondary contact during later range shifts (Lin et al., 2025). Differences in habitat choice may also contribute to the asymmetric gene flow, which is substantially higher from *P. conspicillatus* to *P. alecto*. If *P. alecto* is spreading into rainforest habitats occupied by *P. conspicillatus*, then such a range expansion can lead to asymmetric introgression of local genes into the genome of the encroaching species (Excoffier et al., 2009). Alternatively, asymmetric gene flow can also occur due to asymmetric mating

421 between the sexes, as was found in two closely related horseshoe bat species (Mao et al., 2013).
422 While *P. alecto* and *P. conspicillatus* do not differ substantially in size or morphology (Neaves et
423 al., 2018), asymmetric mating could still occur due to differences in mating behavior and timing.

424 We did not find substantial evidence supporting our hypothesis that *P. alecto* and *P.*
425 *conspicillatus* form an interbreeding population with gradual isolation-by-distance along the
426 geographic ring connecting Australia, Indonesia, and New Guinea. Our findings that Australian
427 populations of the two species interbreed and Indonesian *P. alecto* show strongest isolation-by-
428 distance from New Guinean *P. conspicillatus* superficially supports the hypothesis of a ring
429 species. Although the gene flow we infer between Australia and Indonesia depends on flying-
430 foxes currently making a challenging journey of around 500 km in the present day, bats may use
431 reefs such as Ashmore reef and oil rigs as stepping stones. Historically, dispersal distances
432 during the Pleistocene have also been substantially lower as the Sahul Shelf extending from
433 Australia was exposed during periods of lower sea levels (Karin et al., 2020; Voris, 2000).
434 However, we did not sufficiently sample the hypothesized endpoint of the ring connecting
435 Indonesia to New Guinea to confirm that admixture ceased in this region. Additionally, the
436 substantial divergence between the species on the Australian mainland, despite limited
437 geographic barriers for such mobile animals, suggests that *P. alecto* and *P. conspicillatus* may
438 have diverged in allopatry on the islands of the Indo-Australian Archipelago and later colonized
439 Australia, establishing secondary contact and admixing. Alternatively, divergence could have
440 proceeded through sympatric or parapatric speciation driven by ecological specialization,
441 behavioral isolation, or reproductive barriers accumulating in genomic islands (Ravinet et al.,
442 2017; Richards et al., 2019). Such scenarios of speciation and secondary contact are also
443 supported by our coalescent modelling. Unfortunately, the resolution of biogeographic analyses
444 in flying-foxes is limited and only indicates *P. alecto* and *P. conspicillatus* originated in the
445 broad region of Australia, New Guinea and the South Pacific (Tsang et al., 2020). Based on
446 Bayesian divergence-time estimates, we found *P. alecto* and *P. conspicillatus* diverged in the
447 Pleistocene as recently as 322.4-1023.7 kya. This time was shaped by increases in land area and
448 elevation in Wallacea (Hall, 2013) as well as the uplift of New Guinea ca. 5 mya, which played a
449 key role as an ecological "stepping stone" between Wallacea and the Australian mainland
450 (Roycroft et al., 2022). Notably, Australia and New Guinea were connected at times of low sea
451 level during the Pleistocene including up to ca. 8 kya (Dodson, 1989; Voris, 2000). During the

452 Holocene, human-wildlife conflict (Preece, 2023) and the reduction of rainforest habitat in
453 Australia (Rule et al., 2012) may also have substantially impacted flying-fox distributions. These
454 geographic upheavals provided ample opportunities for speciation, but also complicate
455 reconstruction of flying-fox biogeography to establish the existence of a ring species. Moreover,
456 confirming a ring species requires strong evidence since seemingly clear cases of ring species
457 have been shown to result from more complex scenarios of vicariance, long-distance-
458 colonization and allopatry (Liebers et al., 2004). Extended sampling of the range of *P. alecto* and
459 *P. conspicillatus* outside of Australia combined with morphological analysis and whole genome
460 sequencing could shed further light on the evolutionary origin of these species.

461 Our findings also have implications for conservation management of flying-foxes and pathogen
462 control. *P. conspicillatus* is classified as endangered and hybridization, such as the cases we
463 identified with *P. alecto*, may increase extinction risk (Todesco et al., 2016). However, the
464 asymmetry of the gene flow between the two species, which results in limited admixture in *P.*
465 *conspicillatus* suggests that there is limited increased extinction risk due to hybridization.
466 Furthermore, the constant migration inferred between New Guinea and Australian *P.*
467 *conspicillatus* populations may increase the resilience of the species by maintaining diversity.
468 Unlike *P. conspicillatus*, *P. alecto* is currently listed as "Least Concern" by the International
469 Union for Conservation of Nature (IUCN) across its range. However, the taxon *P. alecto alecto*
470 identified here may be at risk, particularly since Indonesian populations in Sulawesi have
471 declined due to hunting pressure since the 1970s (Sheherazade & Tsang, 2015). Our population
472 genetic findings of high connectivity between flying-fox populations, including across
473 international borders, can also inform studies of pathogen transmission and the management of
474 biosecurity risk (Breed et al., 2010). For example, *P. alecto* has been implicated as a reservoir for
475 bat-borne pathogens including Hendra virus (Edson et al., 2019). The high migration rates we
476 inferred between *P. alecto* populations suggests that emerging viral strains can rapidly spread
477 across the wide distribution of its host. Although these risks are well-understood and mitigated
478 between Australia and New Guinea, our study suggests that transmission between northern
479 Australia and Indonesia is underappreciated. Finally, hybridization between flying-foxes has also
480 been suggested to explain the wide distribution of Nipah virus through interspecies viral
481 transmission (Olival et al., 2020), implying pathogens hosted by *P. alecto* may readily be
482 transmitted and spread by *P. conspicillatus*.

5 Conclusion

We have used genomic markers to provide new insights into the evolutionary history and population dynamics of flying-foxes, revealing high genetic connectivity across Australian populations and high gene flow across disjunct *P. conspicillatus* populations in Australia and New Guinea. The isolation-by-distance observed in Indonesian *P. alecto* contrasts with the weak differentiation across large distances in other populations, highlighting the role of water barriers in shaping genetic structure. While our results do not support a ring species model for *P. alecto* and *P. conspicillatus*, they suggest a complex history of isolation-by-distance and admixture contributing to the evolution of these recently diverged species.

6 Data and code accessibility statement

Raw sequence reads and metadata are deposited in the SRA (BioProject PRJNA1230740). All code and genotype data used for the population genetic analysis and generation of figures is available via github (https://github.com/ascheben/pteropus_popgen_analysis).

7 Ethics approval statement

The animals sampled in this study were captured in accordance with animal ethics approval (Permit number AEC 2016-17).

8 Author contributions

AS: formal analysis, data curation, writing - original draft. **AMcK**: resources, data curation, validation, writing - review and editing. **TW**: resources, data curation, validation, writing - review and editing. **DAW**: conceptualisation, methodology, validation, writing - review and editing, supervision. **SSM**: investigation, writing - review and editing. **EPV**: resources, validation, writing - review and editing. **BLW**: conceptualisation, methodology, validation, writing - review and editing, supervision, funding acquisition.

9 Acknowledgements

This work was funded by the CSIRO Biodiversity, Ecosystem Knowledge and Services Program. We thank Owain Edwards for intellectual input and Samia Elfekih and Ian Cresswell for logistical support. We thank Tolga Bat Hospital, Bat Care Capricornia, Kimberly Wildlife Carers, Western Australian Museum, Port Moresby Botanical Gardens, National Flying-fox monitoring program (NFFMP), Cecelia Sanchez, Chris Todd &Wayne Boardman for assistance in collecting samples. We also thank Christina DeDora and Jesse Ingram for manuscript editing support. Finally, we thank two anonymous reviewers for constructive comments.

10 Conflicts of interest

The authors declare no conflicts of interest.

11 Supplementary figures

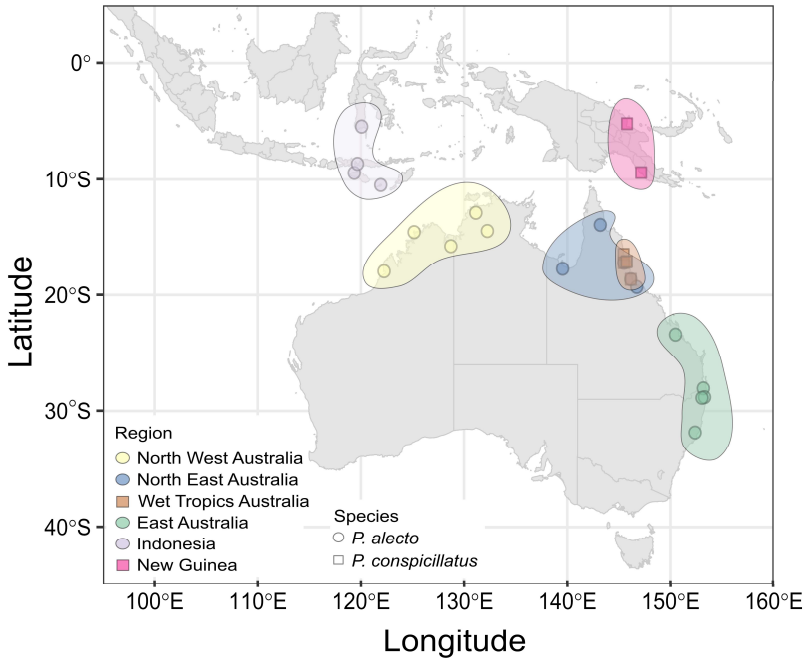

Figure S1. Roost locations and their assignment to distinct geographic regions sampled in this study. To highlight the regions relevant to this study, sampling locations here are shown only for the most widely distributed species *Pteropus alecto* and *P. conspicillatus*.

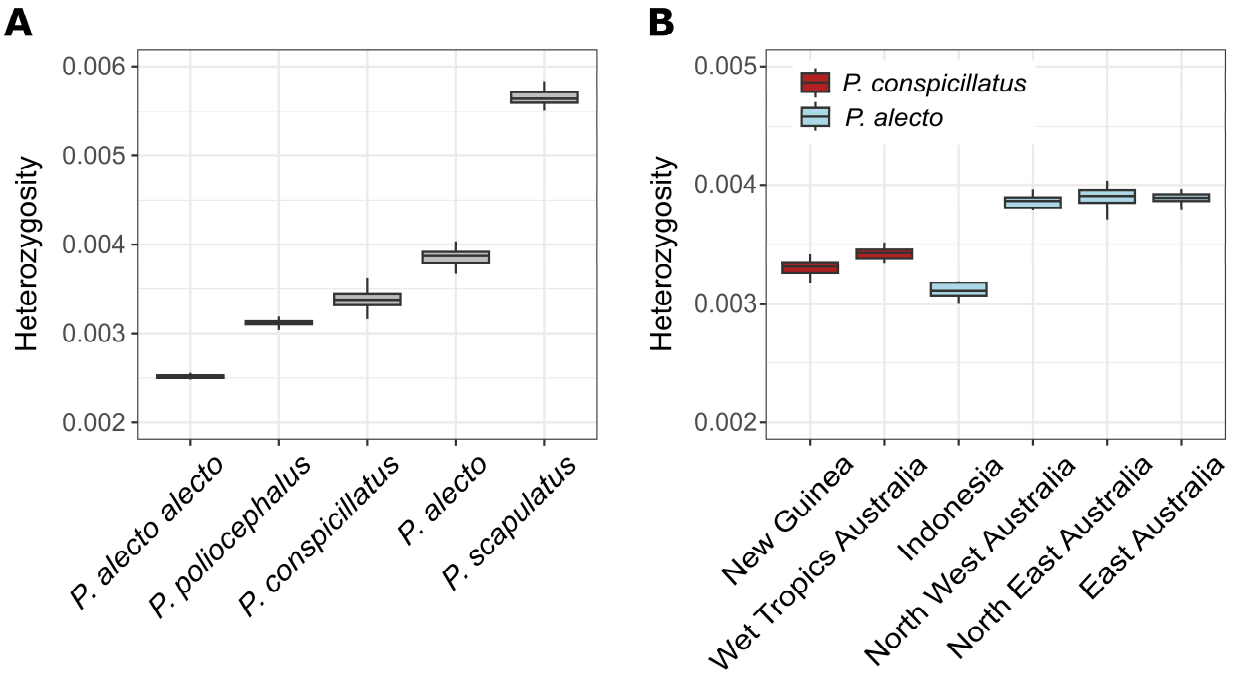

Figure S2. Genome-wide heterozygosity estimates for A) four flying-fox species and B) six regional populations of *Pteropus alecto* and *P. conspicillatus*. A total of 2,024,709 sites were used *Pteropus alecto*, 2,518,218 for *P. conspicillatus*, 2,183,168 for *P. alecto alecto*, 2,610,770 for *P. poliocephalus*, and 2,409,166 for *P. scapulatus*.

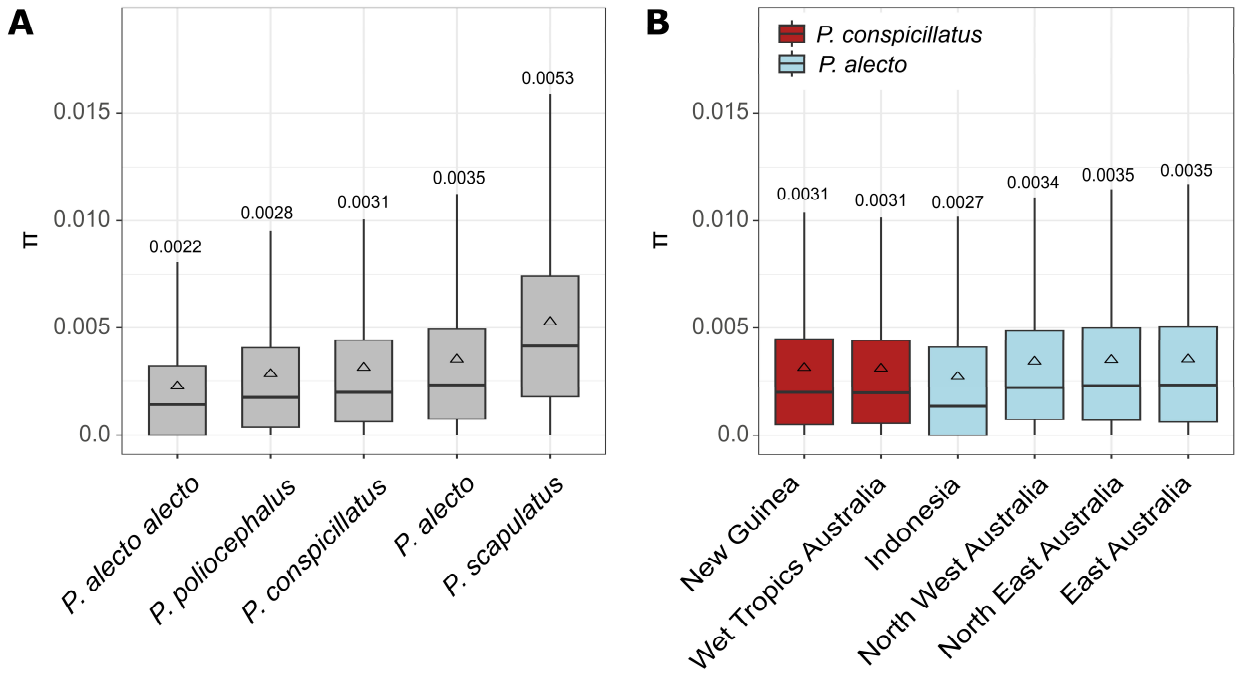

524 **Figure S3**. Genome-wide nucleotide diversity (π) estimates for A) four flying-fox species and B) six
525 regional populations of *Pteropus alecto* and *P. conspicillatus*. Means are shown as triangles and specific
526 mean values are shown above each boxplot. The number of sites used for each species is the same as
527 listed in the Figure S1 legend.

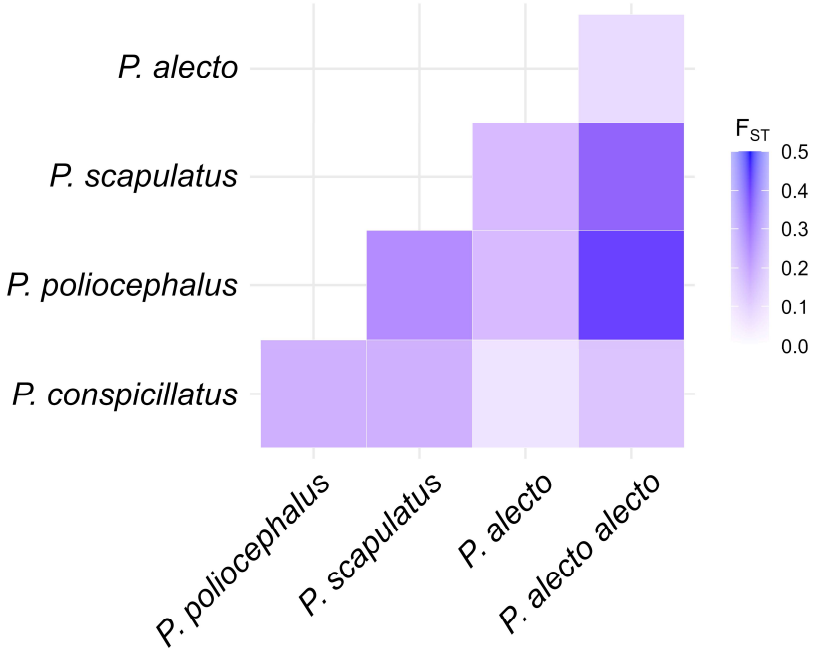

528

529 **Figure S4**. Genetic differentiation between four flying-fox species based on F_{ST}. The genetically distinct
530 Indonesian *P. alecto alecto* group is shown separately.

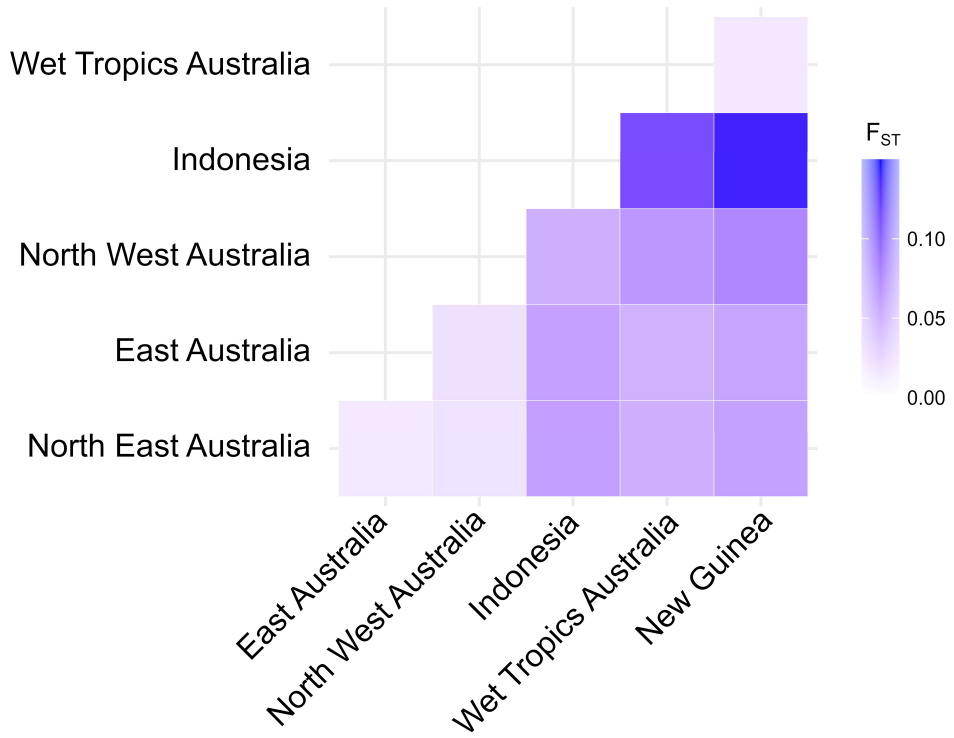

Figure S5. Genetic differentiation between geographic populations of *P. alecto* and *P. conspicillatus* based on F_{ST}. The Wet Tropics Australia and New Guinea groups represent *P. conspicillatus* and the other groups represent *P. alecto*.

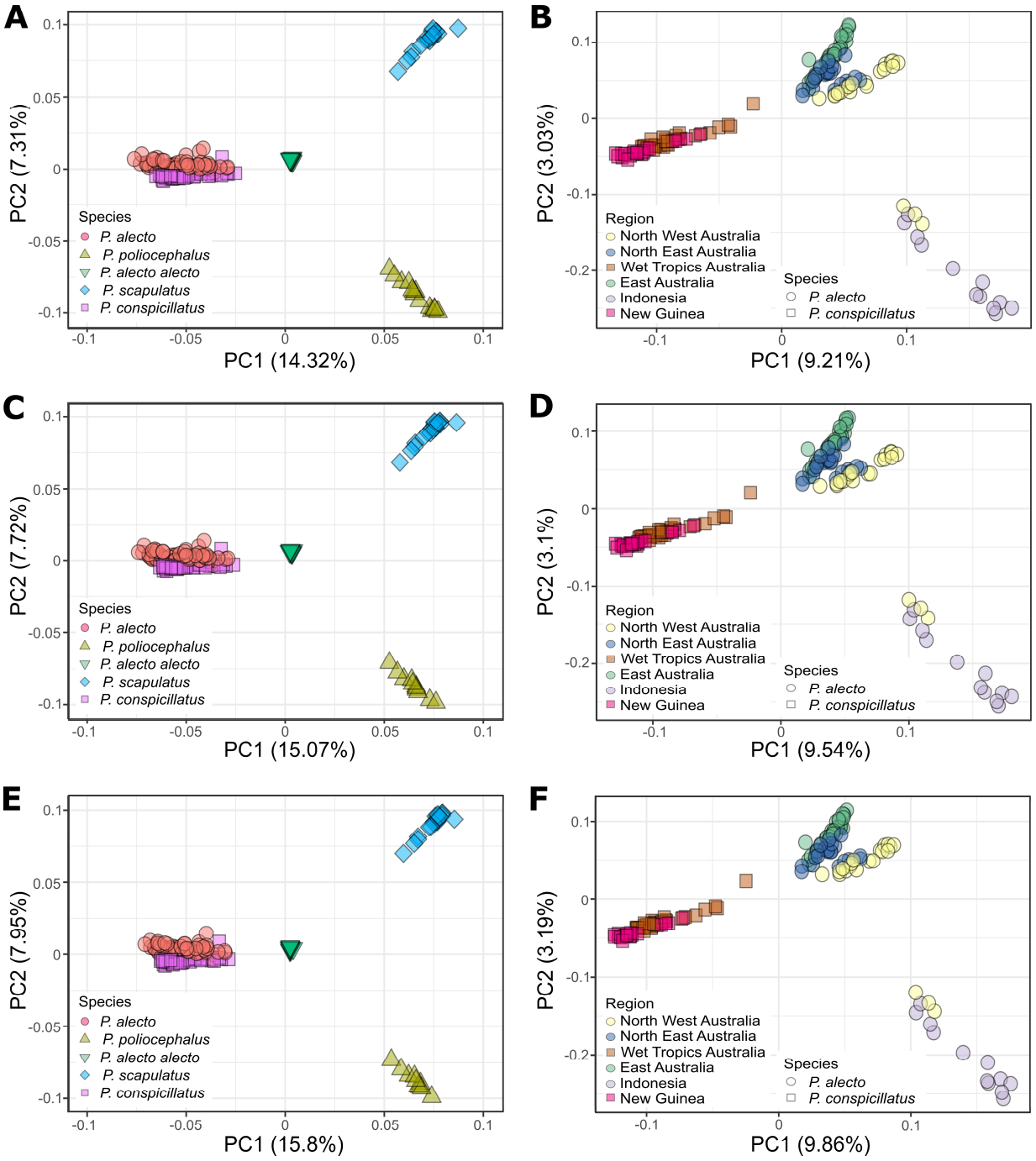

Figure S6. SNP-based principal component analysis (PCA) of flying-fox populations across three genotype missingness thresholds. For the species-level PCA, a genotype missingness threshold of 50% (22,394 SNPs) is shown in A), 40% (19,501 SNPs) in C), and 30% (16,160 SNPs) in E). For the population-level PCA of *P. alecto* and *P. conspicillatus*, a genotype missingness threshold of 50% (33,830 SNPs) is shown in B), 40% (29,222 SNPs) in D), and 30% (23,946 SNPs) in F).

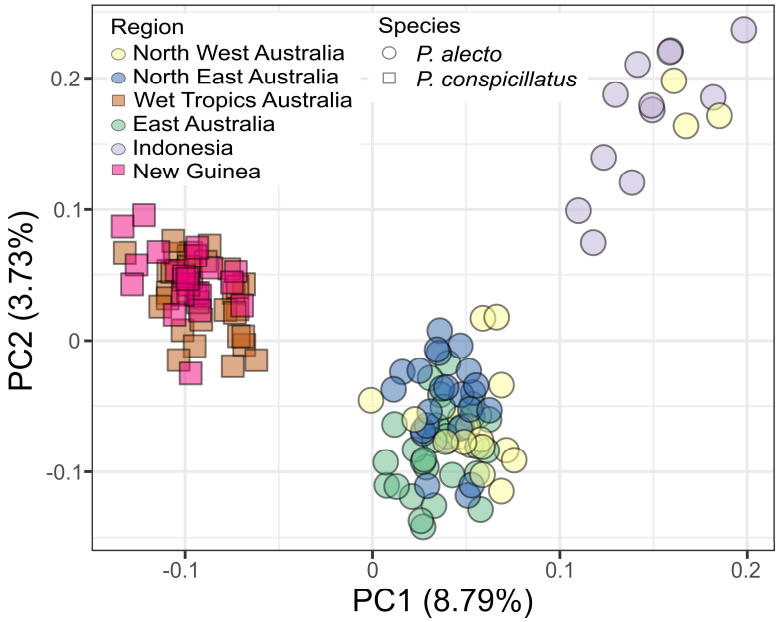

Figure S7. SNP-based principal component analysis (PCA) of *P. alecto* and *P. conspicillatus* populations using 216 SNPs with no missing genotypes.

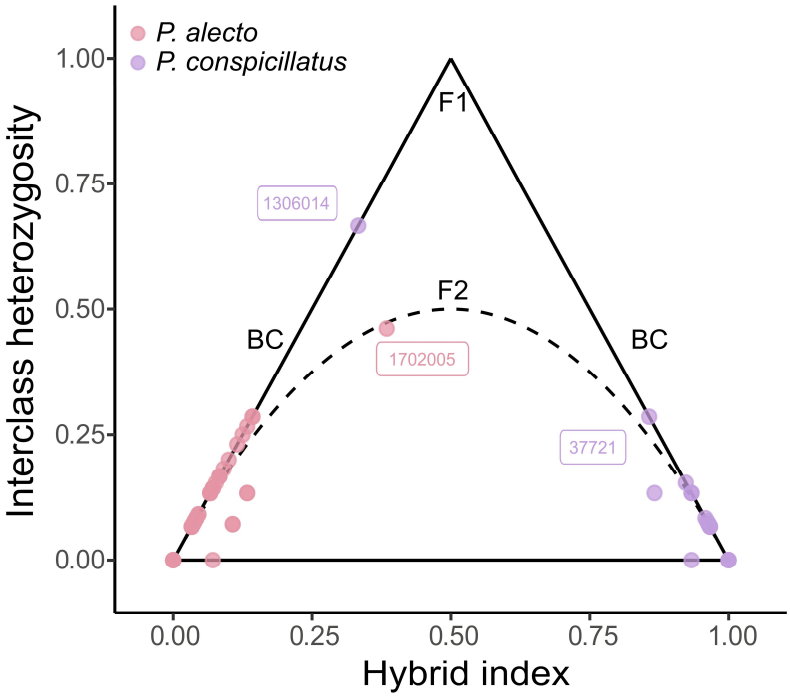

Figure S8. Triangle plot of admixture between *P. alecto* and *P. conspicillatus* individuals based on 15 ancestry-informative SNP markers. The hybrid index of F_1 and F_2 hybrids is expected to be 0.5 while backcross (BC) individuals between hybrids and parental lineages are expected to lie on the edges of the triangle with elevated heterozygosity and hybrid indices. Proportions of missing SNP markers were not associated with high interclass heterozygosity or hybrid indices (Figure S9).

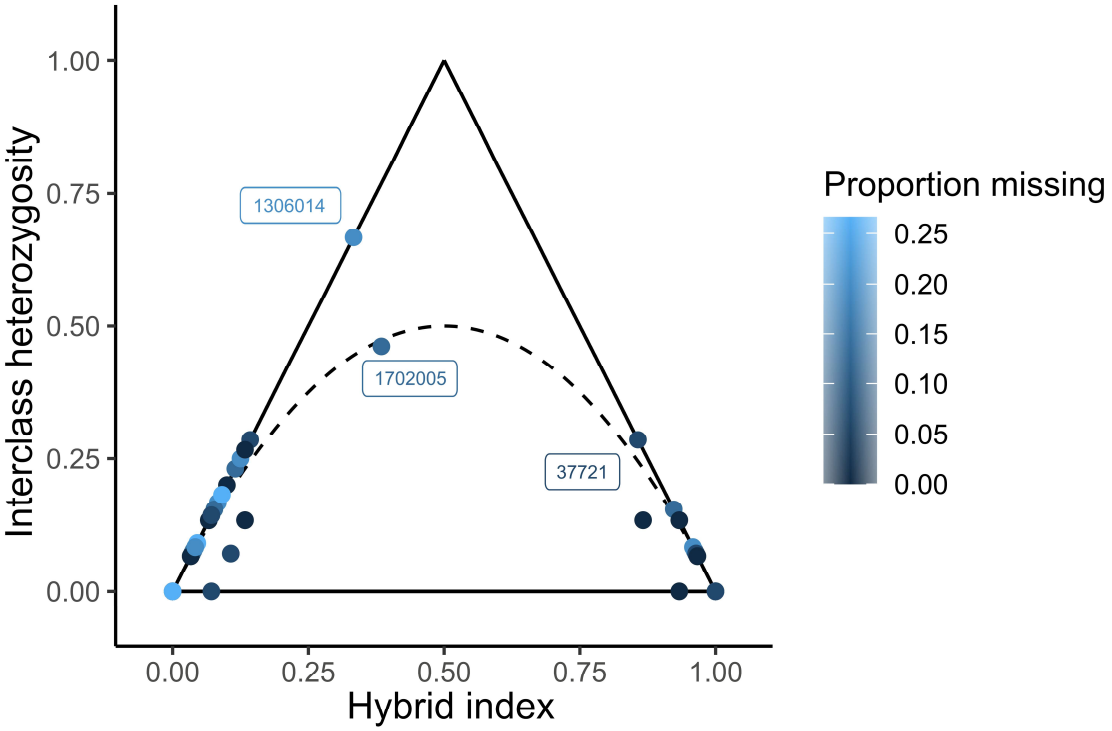

546 **Figure S9**. Triangle plot of admixture between *P. alecto* and *P. conspicillatus* individuals based on 15
547 ancestry-informative SNP markers colored by the proportion of missing markers per individual.

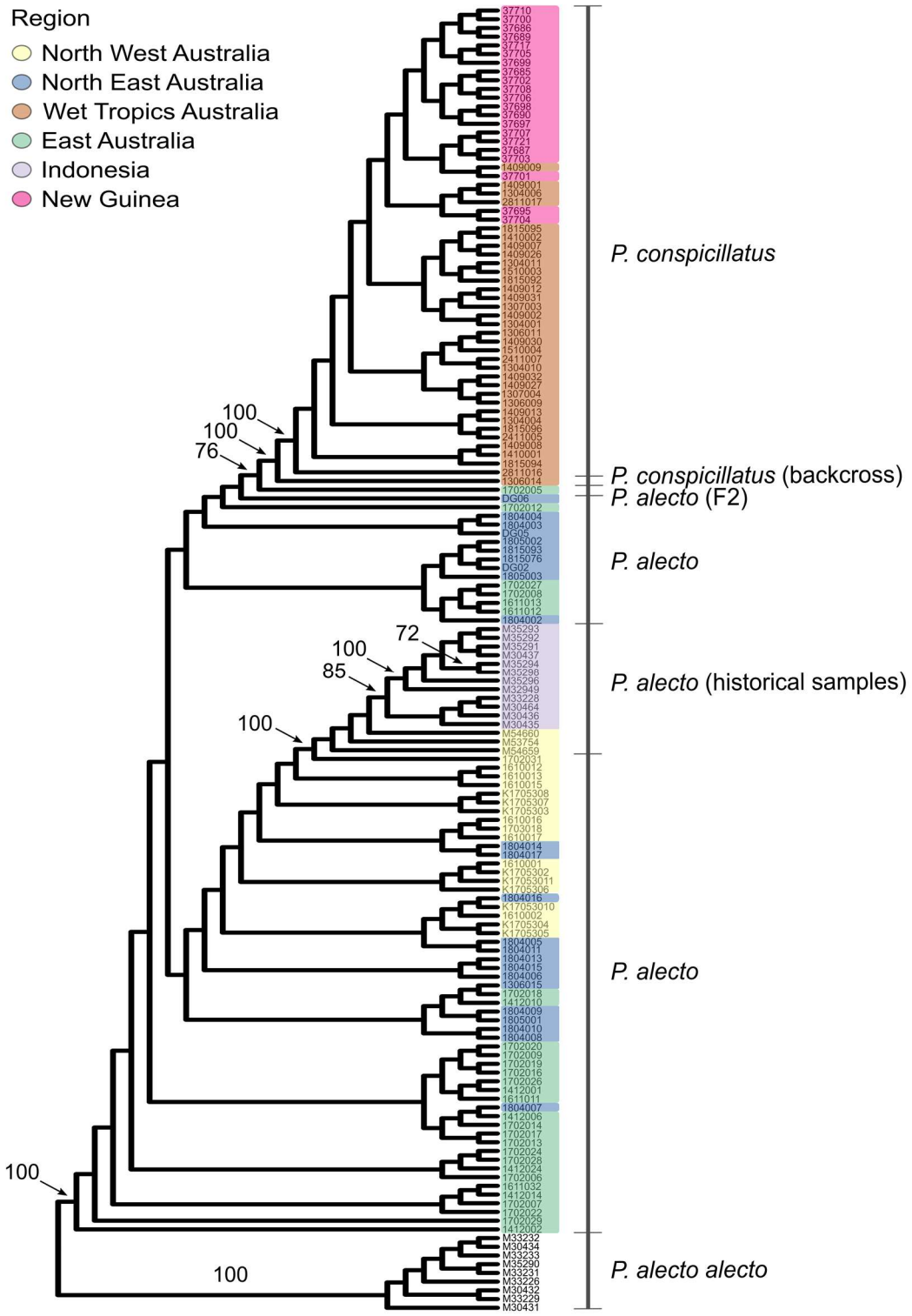

Figure S10. SNP-based maximum likelihood phylogeny of *Pteropus alecto* and *P. conspicillatus*. A total of 17,708 SNP sites were used. Individuals are highlighted in a color by geographic region and the Indonesian *P. alecto alecto* group is used as the outgroup. Historical *P. alecto* samples were collected from 1989 to 2003 (see Table S1). Bootstrap support values >70 are shown.

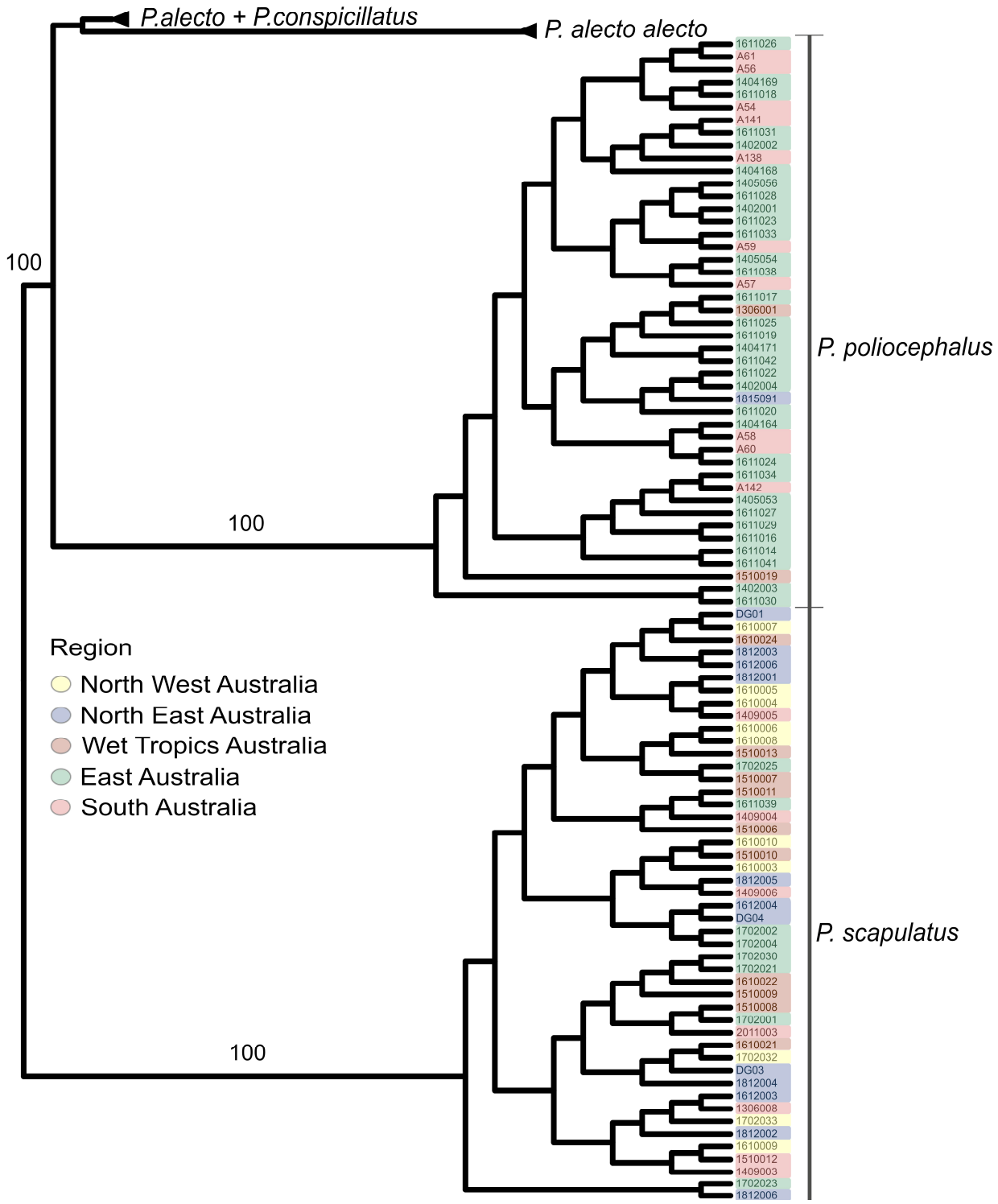

Figure S11. SNP-based maximum likelihood phylogeny of *Pteropus poliocephalus* and *P. scapulatus*. A total of 11,818 SNP sites were used. Individuals are highlighted in a color by geographic region. Bootstrap support values >70 are shown, highlighting robustly supported branches.

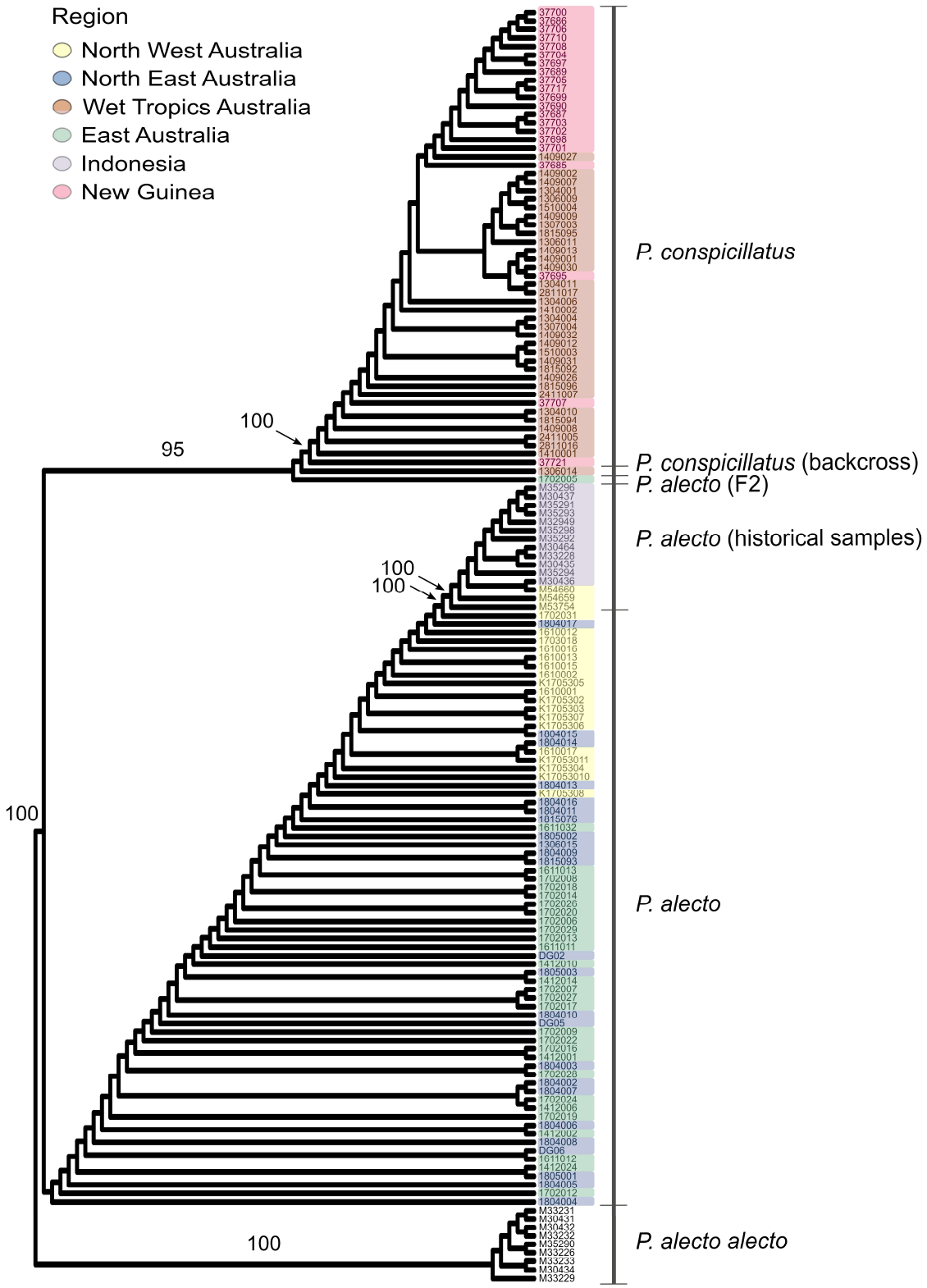

Figure S12. SNP-based phylogeny of *Pteropus alecto* and *P. conspicillatus* inferred by CASTER-site. A total of 17,708 SNP sites were used. Individuals are highlighted in a color by geographic region. Branch bootstrap support values >95 are shown.

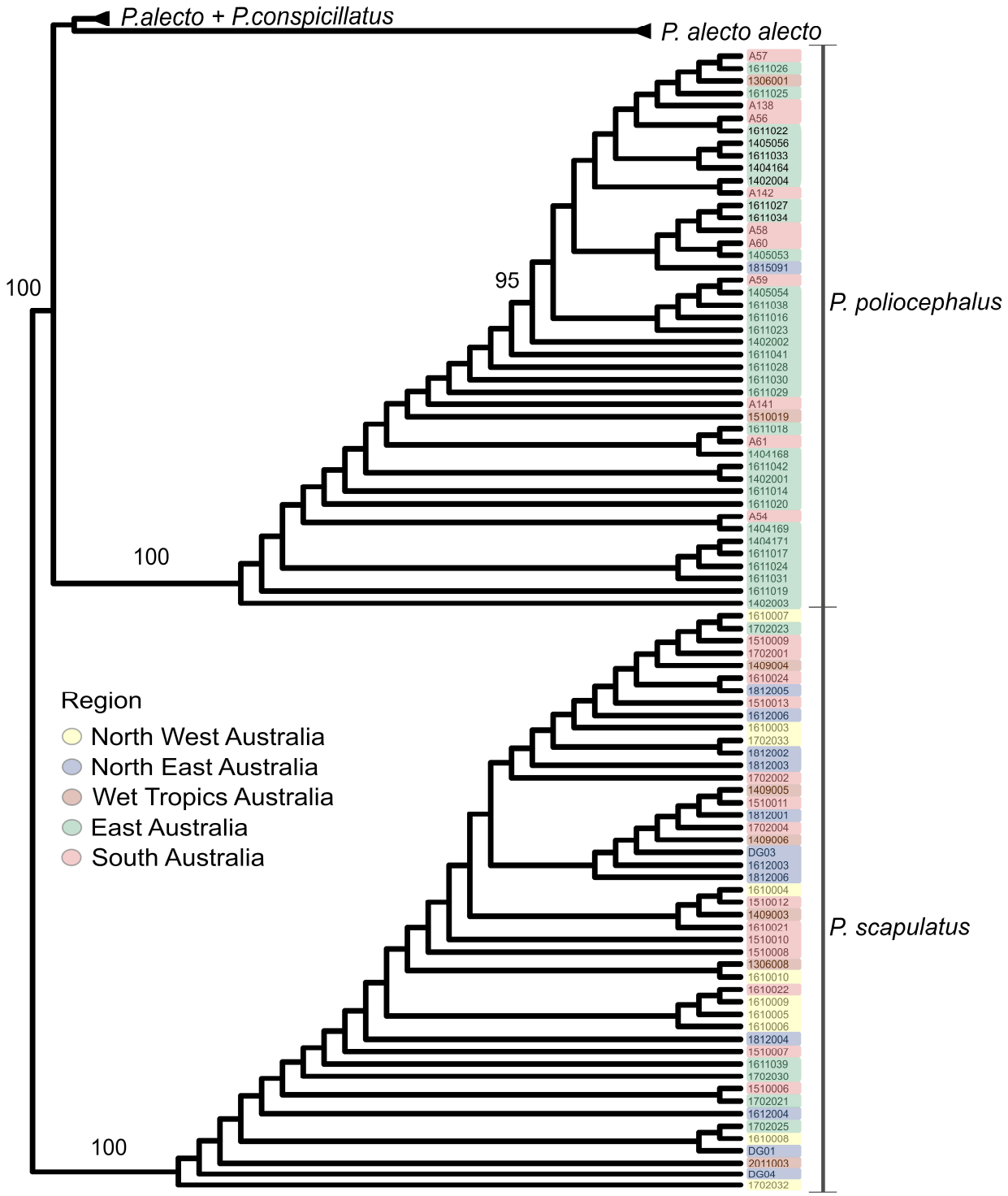

Figure S13. SNP-based phylogeny of *Pteropus poliocephalus* and *P. scapulatus* inferred by CASTER-site. A total of 11,818 SNP sites were used. Individuals are highlighted in a color by geographic region. Branch bootstrap support values >95 are shown.

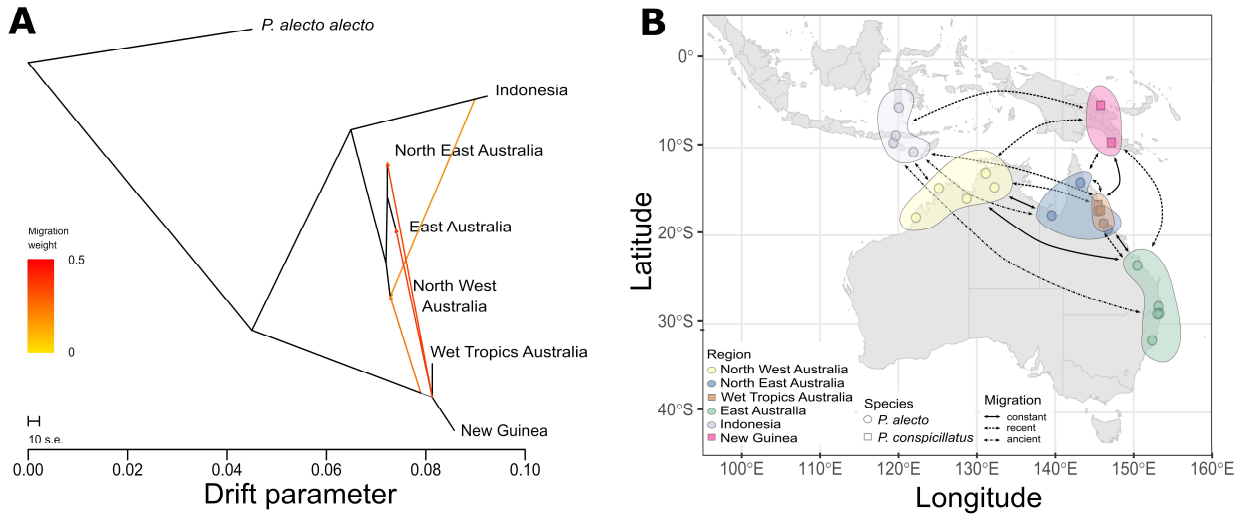

Figure S14. Gene flow in *Pteropus alecto* and *P. conspicillatus* along a geographic ring ranging across Indonesia, Australia, and New Guinea. A) Maximum likelihood tree with migration edges for six *P. alecto* and *P. conspicillatus* populations. *P. conspicillatus* populations include New Guinea and Wet Tropics Australia, the remainder are *P. alecto* populations. The Indonesian *P. alecto alecto* was used as the outgroup. B). Map of inferred migration scenarios between populations using coalescent simulations. Only recent and constant migrations are shown (see Table S9 for additional inferred parameters).

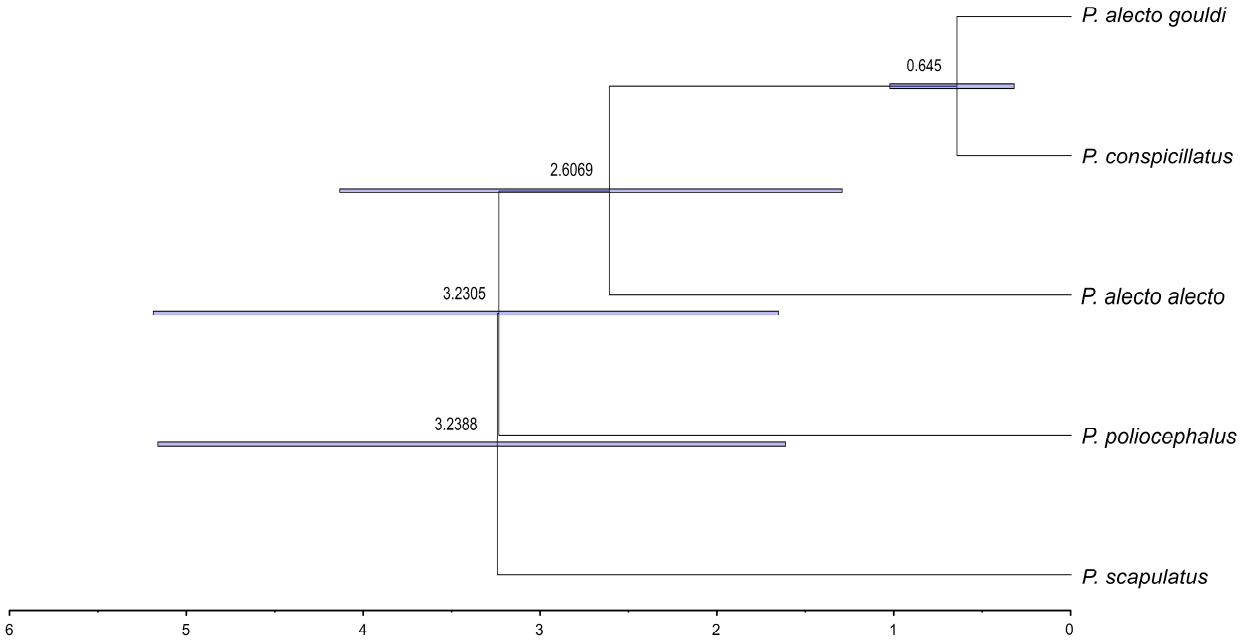

Figure S15. Dated phylogeny of sampled flying-fox species inferred using BEAST and SNAPP from genome-wide SNPs for three samples per branch. Mean divergence estimates per node are ages in millions of years before present. Blue bars show the 95% highest posterior density interval for each node. The subspecies designation *Pteropus alecto gouldi*, used to describe Australian *P. alecto*, is used here to indicate that the three sampled individuals for this branch all originate from Australia.

12 References

Abbott, R., Albach, D., Ansell, S., Arntzen, J. W., Baird, S. J. E., Bierne, N., Boughman, J., Brelsford, A., Buerkle, C. A., Buggs, R., Butlin, R. K., Dieckmann, U., Eroukhmanoff, F., Grill, A., Cahan, S. H., Hermansen, J. S., Hewitt, G., Hudson, A. G., Jiggins, C., … Zinner, D. (2013). Hybridization and speciation. *Journal of Evolutionary Biology*, *26*(2), 229–246. https://doi.org/10.1111/j.1420-9101.2012.02599.x

Aguillon, S. M., Fitzpatrick, J. W., Bowman, R., Schoech, S. J., Clark, A. G., Coop, G., & Chen, N. (2017). Deconstructing isolation-by-distance: The genomic consequences of limited dispersal. *PLoS Genetics*, *13*(8), e1006911. https://doi.org/10.1371/journal.pgen.1006911

Alcaide, M., Scordato, E. S., Price, T. D., & Irwin, D. E. (2014). Genomic divergence in a ring species complex. Nature, 511(7507), 83-85. https://doi.org/10.1038/nature13285

Almeida, F. C., Simmons, N. B. & Giannini, N. P. (2020). A species-level phylogeny of Old World fruit bats with a new higher-level classification of the family Pteropodidae. *American Museum Novitates*, 3950, 1–24. https://doi.org/10.1206/3950.1

Almeida, F. C., Giannini, N. P., DeSalle, R., & Simmons, N. B. (2009). The phylogenetic relationships of cynopterine fruit bats (Chiroptera: Pteropodidae: Cynopterinae). *Molecular Phylogenetics and Evolution*, *53*(3), 772–783. https://doi.org/10.1016/j.ympev.2009.07.035

Almeida, F. C., Giannini, N. P., Simmons, N. B., & Helgen, K. M. (2014). Each flying fox on its own branch: A phylogenetic tree for *Pteropus* and related genera (Chiroptera: Pteropodidae). *Molecular Phylogenetics and Evolution*, *77*, 83–95. https://doi.org/10.1016/j.ympev.2014.03.009

Andersen, K. (1912). Catalogue of the Chiroptera in the collection of the British Museum. Volume I: Megachiroptera. British Museum (Natural History), London.

Breed, A. C., Field, H. E., Smith, C. S., Edmonston, J., & Meers, J. (2010). Bats without borders: long-distance movements and implications for disease risk management. *Ecohealth*, *7*(2), 204–212. https://doi.org/10.1007/s10393-010-0332-z

Bruxaux, J., Zhao, W., Hall, D., Curtu, A. L., Androsiuk, P., Drouzas, A. D., Gailing, O., Konrad, H., Sullivan, A. R., Semerikov, V., & Wang, X.-R. (2024). Scots pine—Panmixia and the elusive signal of genetic adaptation. *The New Phytologist*, *243*(3), 1231–1246. https://doi.org/10.1111/nph.19563

Chang, C. C., Chow, C. C., Tellier, L. C., Vattikuti, S., Purcell, S. M., & Lee, J. J. (2015). Second-generation PLINK: Rising to the challenge of larger and richer datasets. *GigaScience*, *4*(1), s13742-015-0047–0048. https://doi.org/10.1186/s13742-015-0047-8

Chen, S.-F., Juan, C.-H., Rossiter, S. J., Kinjo, T., Fukui, D., Kawai, K., Tsang, S. M., Veluz, M. J., Sakurai, H., Lin, H.-C., Jang-Liaw, N.-H., Osawa, K., Ko, W.-Y., & Izawa, M. (2021). Population genetic structure of the insular Ryukyu flying fox *Pteropus dasymallus*. *Biotropica*, *53*(2), 548–559. https://doi.org/10.1111/btp.12897

Cho, Y. S., Hu, L., Hou, H., Lee, H., Xu, J., Kwon, S., Oh, S., Kim, H.-M., Jho, S., Kim, S., Shin, Y.-A., Kim, B. C., Kim, H., Kim, C., Luo, S.-J., Johnson, W. E., Koepfli, K.-P., Schmidt-Küntzel, A., Turner, J. A., … Bhak, J. (2013). The tiger genome and comparative analysis with lion and snow leopard genomes. *Nature Communications*, *4*(1), 2433. https://doi.org/10.1038/ncomms3433

DaCosta, J. M., & Sorenson, M. D. (2014). Amplification biases and consistent recovery of loci in a double-digest RAD-seq protocol. *PloS One*, 9(9), e106713.

https://doi.org/10.1371/journal.pone.0106713

Danecek, P., Auton, A., Abecasis, G., Albers, C. A., Banks, E., DePristo, M. A., Handsaker, R. E., Lunter, G., Marth, G. T., Sherry, S. T., McVean, G., & Durbin, R. (2011). The variant call format and VCFtools. *Bioinformatics*, *27*(15), 2156–2158. https://doi.org/10.1093/bioinformatics/btr330

Danecek, P., Bonfield, J. K., Liddle, J., Marshall, J., Ohan, V., Pollard, M. O., Whitwham, A., Keane, T., McCarthy, S. A., Davies, R. M., & Li, H. (2021). Twelve years of SAMtools and BCFtools. *GigaScience*, *10*(2), giab008. https://doi.org/10.1093/gigascience/giab008

Dodson, J. R. (1989). Late pleistocene vegetation and environmental shifts in Australia and their bearing on faunal extinctions. *Journal of Archaeological Science*, *16*(2), 207–217. https://doi.org/10.1016/0305-4403(89)90066-6

Eby, P. (1991). Seasonal movements of grey-headed flying-foxes, *Pteropus poliocephalus* (Chiroptera: Pteropodidae), from two maternity camps in northern New South Wales. *Wildlife Research*, *18*(5), 547–559. https://doi.org/10.1071/wr9910547

Edson, D., Peel, A. J., Huth, L., Mayer, D. G., Vidgen, M. E., McMichael, L., Broos, A., Melville, D., Kristoffersen, J., Jong, C. de, McLaughlin, A., & Field, H. E. (2019). Time of year, age class and body condition predict Hendra virus infection in Australian black flying foxes (*Pteropus alecto*). *Epidemiology & Infection*, *147*, e240. https://doi.org/10.1017/S0950268819001237

Excoffier, L., Dupanloup, I., Huerta-Sánchez, E., Sousa, V. C., & Foll, M. (2013). Robust demographic inference from genomic and SNP data. *PLoS Genetics*, *9*(10), e1003905. https://doi.org/10.1371/journal.pgen.1003905

Excoffier, L., Foll, M., & Petit, R. J. (2009). Genetic consequences of range expansions. *Annual Review of Ecology, Evolution, and Systematics*, *40*, 481–501. https://doi.org/10.1146/annurev.ecolsys.39.110707.173414

Fitak, R. R. (2021). OptM: Estimating the optimal number of migration edges on population trees using Treemix. *Biology Methods and Protocols*, *6*(1), bpab017. https://doi.org/10.1093/biomethods/bpab017

Fox, S. (2006). Population structure in the spectacled flying fox, *Pteropus conspicillatus*: A study of genetic and demographic factors. PhD thesis, James Cook University. https://researchonline.jcu.edu.au/8053/

Gutenkunst, R. N., Hernandez, R. D., Williamson, S. H., & Bustamante, C. D. (2009). Inferring the joint demographic history of multiple populations from multidimensional SNP frequency data. *PLoS Genetics*, *5*(10), e1000695. https://doi.org/10.1371/journal.pgen.1000695

Hall, R. (2013). The palaeogeography of Sundaland and Wallacea since the Late Jurassic. *Journal of Limnology*, *72*(s2). https://doi.org/10.4081/jlimnol.2013.s2.e1

He, H., Yang, H., Foo, R., Chan, W., Zhu, F., Liu, Y., Zhou, X., Ma, L., Wang, L.-F., & Zhai, W. (2023). Population genomic analysis reveals distinct demographics and recent adaptation in the black flying fox (*Pteropus alecto*). *Journal of Genetics and Genomics*, *50*(8), 554–562. https://doi.org/10.1016/j.jgg.2023.05.002

Irwin, D. E., Bensch, S., Irwin, J. H., & Price, T. D. (2005). Speciation by distance in a ring species. *Science*, *307*(5708), 414–416. https://doi.org/10.1126/science.1105201

Karin, B. R., Stubbs, A. L., Arifin, U., Iskandar, D. T., Arida, E., Austin, C. C., & McGuire, J. A. (2020). Crossing Lydekker's line: Northern Water Dragons (*Tropicagama temporalis*) colonized the Mollucan Islands of Indonesia from New Guinea. *Herpetologica*, *76*(3), 344–350. https://doi.org/10.1655/Herpetologica-D-19-00033

Korunes, K. L., & Samuk, K. (2021). pixy: Unbiased estimation of nucleotide diversity and divergence in the presence of missing data. *Molecular Ecology Resources*, *21*(4), 1359–1368. https://doi.org/10.1111/1755-0998.13326

Kuchta, S. R., & Wake, D. B. (2016). Wherefore and whither the ring species? *Copeia*, 104(1), 189-201.

Larsen, P. A., Hayes, C. E., Wilkins, M. A., Gomard, Y., Sookhareea, R., Yoder, A. D., & Goodman, S. M. (2014). Population genetics of the Mauritian flying fox, *Pteropus niger*. *Acta Chiropterologica*, *16*(2), 293–300. https://doi.org/10.3161/150811014X687251

Li, H. (2013). Aligning sequence reads, clone sequences and assembly contigs with BWA-MEM. *arXiv*. https://doi.org/10.48550/arXiv.1303.3997

Liebers, D., de Knijff, P., & Helbig, A. J. (2004). The herring gull complex is not a ring species. *Proceedings of the Royal Society B: Biological Sciences*, *271*(1542), 893–901. https://doi.org/10.1098/rspb.2004.2679

Lin, T.-H., Shen, Z.-Y., Chou, M.-H., Sun, P.-W., Shen, C.-C., Huang, J.-P., & Lin, S.-M. (2025). Allopatric speciation and interspecific gene flow driven by niche conservatism of *Diploderma* tree lizards in Taiwan. *Molecular Ecology*, e17718. https://doi.org/10.1111/mec.17718

Lomolino, M. V. (2000). A call for a new paradigm of island biogeography. *Global Ecology and Biogeography*, *9*(1), 1–6. https://doi.org/10.1046/j.1365-2699.2000.00185.x

Macdonald, S. L., Bradford, M., McKeown, A., Vanderduys, E., Hoskins, A., & Westcott, D. (2021). Camp site habitat preferences of the little red flying-fox (*Pteropus scapulatus*) in Queensland. *Australian Journal of Zoology*,*68*, 234–253. https://doi.org/10.1071/ZO20079

Manichaikul, A., Mychaleckyj, J. C., Rich, S. S., Daly, K., Sale, M., & Chen, W.-M. (2010). Robust relationship inference in genome-wide association studies. *Bioinformatics*, *26*(22), 2867–2873. https://doi.org/10.1093/bioinformatics/btq559

Mao, X., Thong, V. D., Bates, P. J. J., Jones, G., Zhang, S., & Rossiter, S. J. (2013). Multiple cases of asymmetric introgression among horseshoe bats detected by phylogenetic conflicts across loci. *Biological Journal of the Linnean Society*, *110*(2), 346–361. https://doi.org/10.1111/bij.12138

Marcus, J., Ha, W., Barber, R. F., & Novembre, J. (2021). Fast and flexible estimation of effective migration surfaces. *eLife*, *10*, e61927. https://doi.org/10.7554/eLife.61927

McIlwee, A. P., & Martin, L. (2014). On the intrinsic capacity for increase of Australian flying-foxes (*Pteropus* spp., Megachiroptera). *Australian Zoologist*, *32*(1), 76–100. https://doi.org/10.7882/AZ.2002.008

Nachman, M. W., & Crowell, S. L. (2000). Estimate of the mutation rate per nucleotide in humans. *Genetics*, *156*(1), 297–304. https://doi.org/10.1093/genetics/156.1.297

Neaves, L. E., Danks, M., Lott, M. J., Dennison, S., Frankham, G. J., King, A., Eldridge, M. D. B., Johnson, R. N., & Divljan, A. (2018). Unmasking the complexity of species identification in Australasian flying-foxes. *PLoS One*, *13*(4), e0194908. https://doi.org/10.1371/journal.pone.0194908

Neethling, M., Matthee, C. A., Bowie, R. C., & von der Heyden, S. (2008). Evidence for panmixia despite barriers to gene flow in the southern African endemic, *Caffrogobius caffer* (Teleostei: Gobiidae). *BMC Evolutionary Biology*, *8*(1), 325. https://doi.org/10.1186/1471-2148-8-325

O'Brien, J., Mariani, C., Olson, L., Russell, A. L., Say, L., Yoder, A. D., & Hayden, T. J. (2009). Multiple colonisations of the western Indian Ocean by *Pteropus* fruit bats (Megachiroptera: Pteropodidae): The furthest islands were colonised first. *Molecular Phylogenetics and Evolution*, *51*(2), 294–303. https://doi.org/10.1016/j.ympev.2009.02.010

Olival, K. J., Latinne, A., Islam, A., Epstein, J. H., Hersch, R., Engstrand, R. C., Gurley, E. S., Amato, G., Luby, S. P., & Daszak, P. (2020). Population genetics of fruit bat reservoir informs the dynamics, distribution and diversity of Nipah virus. *Molecular Ecology*, *29*(5), 970–985. https://doi.org/10.1111/mec.15288

Palmer, C., Price, O., & Bach, C. (2000). Foraging ecology of the black flying fox (*Pteropus alecto*) in the seasonal tropics of the Northern Territory, Australia. *Wildlife Research*, *27*(2), 169–178. https://doi.org/10.1071/wr97126

Parsons, J. G., Cairns, A., Johnson, C. N., Robson, S. K. A., Shilton, L. A., & Westcott, D. A. (2007). Dietary variation in spectacled flying foxes (*Pteropus conspicillatus*) of the Australian Wet Tropics. *Australian Journal of Zoology*, *54*(6), 417–428. https://doi.org/10.1071/ZO06092

Peel, A. J., Sargan, D. R., Baker, K. S., Hayman, D. T. S., Barr, J. A., Crameri, G., Suu-Ire, R., Broder, C. C., Lembo, T., Wang, L.-F., Fooks, A. R., Rossiter, S. J., Wood, J. L. N., & Cunningham, A. A. (2013). Continent-wide panmixia of an African fruit bat facilitates transmission of potentially zoonotic viruses. *Nature Communications*, *4*(1), 2770. https://doi.org/10.1038/ncomms3770

Pickrell, J. K., & Pritchard, J. K. (2012). Inference of population splits and mixtures from genome-wide allele frequency data. *PLoS Genetics*, *8*(11), e1002967. https://doi.org/10.1371/journal.pgen.1002967

Preece, N. (2023). Spectacled Flying-fox conflicts—Tucker, totem, taunt and threat. *Integrative Conservation*, *2*(3), 112–118. https://doi.org/10.1002/inc3.26

Raj, A., Stephens, M., & Pritchard, J. K. (2014). fastSTRUCTURE: Variational inference of population structure in large SNP data sets. *Genetics*, *197*(2), 573–589. https://doi.org/10.1534/genetics.114.164350

Ravinet, M., Faria, R., Butlin, R. K., Galindo, J., Bierne, N., Rafajlović, M., Noor, M. A. F., Mehlig, B. & Westram, A. M. (2017). Interpreting the genomic landscape of speciation: a road map for finding barriers to gene flow. *Journal of Evolutionary Biology*, 30(8), 1450-1477. https://doi.org/10.1111/jeb.13047

Reich, M. S., Shipilina, D., Talla, V., Bahleman, F., Kébé, K., Berger, J. L., Backström, N., Talavera, G., & Bataille, C. P. (2024). Isotope geolocation and population genomics in *Vanessa cardui*: Short- and long-distance migrants are genetically undifferentiated. *bioRxiv*. https://doi.org/10.1101/2023.12.10.569105

Reudink, M., Kyle, C., Nocera, J. J., Oomen, R. A., Green, M. C., & Somers, C. M. (2011). Panmixia on a continental scale in a widely distributed colonial waterbird. *Biological Journal of the Linnean Society*, *102*(3), 583–592. https://doi.org/10.1111/j.1095-8312.2010.01608.x

Richards, G. C. (1990). The spectacled flying-fox, *Pteropus conspicillatus* (Chiroptera: Pteropodidae), in north Queensland. 2. Diet, seed dispersal and feeding ecology. *Australian Mammalogy*, *13*(1), 25–31. https://doi.org/10.1071/am90004

Richards, E. J., Servedio, M. R., & Martin, C. H. (2019). Searching for sympatric speciation in the genomic era. *BioEssays*, 41(7), 1900047. https://doi.org/10.1002/bies.201900047

Roberts, B. J., Eby, P., & Westcott, D. A. (2020). *Pteropus conspicillatus.* The IUCN Red List of Threatened Species 2020: E.T18721A22080456. https://dx.doi.org/10.2305/IUCN.UK.2020-3.RLTS.T18721A22080456.en

Roberts, B. J., Catterall, C. P., Eby, P., & Kanowski, J. (2012). Long-distance and frequent movements of the flying-fox *Pteropus poliocephalus*: Implications for management. *PLoS One*, *7*(8), e42532. https://doi.org/10.1371/journal.pone.0042532

Rochette, N. C., Rivera-Colón, A. G., & Catchen, J. M. (2019). Stacks 2: Analytical methods for paired-end sequencing improve RADseq-based population genomics. *Molecular Ecology*, *28*(21), 4737–4754. https://doi.org/10.1111/mec.15253

Roycroft, E., Fabre, P.-H., MacDonald, A. J., Moritz, C., Moussalli, A., & Rowe, K. C. (2022). New Guinea uplift opens ecological opportunity across a continent. *Current Biology*, *32*(19), 4215-4224.e3. https://doi.org/10.1016/j.cub.2022.08.021

Rule, S., Brook, B. W., Haberle, S. G., Turney, C. S. M., Kershaw, A. P., & Johnson, C. N. (2012). The aftermath of megafaunal extinction: Ecosystem transformation in Pleistocene Australia. *Science*, *335*(6075), 1483–1486. https://doi.org/10.1126/science.1214261

Sharbel, T. F., Haubold, B., & Mitchell-Olds, T. (2000). Genetic isolation by distance in *Arabidopsis thaliana*: Biogeography and postglacial colonization of Europe. *Molecular Ecology*, *9*(12), 2109–2118. https://doi.org/10.1046/j.1365-294X.2000.01122.x

Shastry, V., Musiani, M., & Novembre, J. (2025). Jointly representing long-range genetic similarity and spatially heterogeneous isolation-by-distance. *bioRxiv*. https://doi.org/10.1101/2025.02.10.637386

Sheherazade, & Tsang, S. M. (2015). Quantifying the bat bushmeat trade in North Sulawesi, Indonesia, with suggestions for conservation action. *Global Ecology and Conservation*, *3*, 324–330. https://doi.org/10.1016/j.gecco.2015.01.003

Simmons, N. B., & Cirranello, A. L. (2025). Bat Species of the World: A taxonomic and geographic database. Version 1.7. https://batnames.org/

Smyčka, J., Toszogyova, A., & Storch, D. (2023). The relationship between geographic range size and rates of species diversification. *Nature Communications*, *14*(1), 5559. https://doi.org/10.1038/s41467-023-41225-6

Sovic, M. G., Carstens, B. C., & Gibbs, H. L. (2016). Genetic diversity in migratory bats: Results from RADseq data for three tree bat species at an Ohio windfarm. *PeerJ*, *4*, e1647. https://doi.org/10.7717/peerj.1647

Stamatakis, A. (2014). RAxML version 8: A tool for phylogenetic analysis and post-analysis of large phylogenies. *Bioinformatics*, *30*(9), 1312–1313. https://doi.org/10.1093/bioinformatics/btu033

Todesco, M., Pascual, M. A., Owens, G. L., Ostevik, K. L., Moyers, B. T., Hübner, S., Heredia, S. M., Hahn, M. A., Caseys, C., Bock, D. G., & Rieseberg, L. H. (2016). Hybridization and extinction. *Evolutionary Applications*, *9*(7), 892–908. https://doi.org/10.1111/eva.12367

Tsang, S. M. (2015). Phylogeography of Southeast Asian flying foxes (Chiroptera: Pteropodidae: *Pteropus*). PhD thesis, City University of New York. https://academicworks.cuny.edu/gc_etds/1161

Tsang, S. M., Wiantoro, S., Veluz, M. J., Simmons, N. B., & Lohman, D. J. (2018). Low levels of population structure among geographically distant populations of *Pteropus vampyrus* (Chiroptera: Pteropodidae). *Acta Chiropterologica*, *20*(1), 59–71. https://doi.org/10.3161/15081109ACC2018.20.1.004

Tsang, S. M., Wiantoro, S., Veluz, M. J., Sugita, N., Nguyen, Y.-L., Simmons, N. B., & Lohman, D. J. (2020). Dispersal out of Wallacea spurs diversification of *Pteropus* flying foxes, the world's largest bats (Mammalia: Chiroptera). *Journal of Biogeography*, *47*(2), 527–537. https://doi.org/10.1111/jbi.13750

Vanderduys, E. P., Caley, P., McKeown, A., Martin, J. M., Pavey, C., & Westcott, D. (2024). Population trends in the vulnerable grey-headed flying-fox, *Pteropus poliocephalus*; results from a long-

term, range-wide study. *PLoS One*, *19*(3), e0298530. https://doi.org/10.1371/journal.pone.0298530

Voris, H. K. (2000). Maps of Pleistocene sea levels in Southeast Asia: Shorelines, river systems and time durations. *Journal of Biogeography*, *27*(5), 1153–1167. https://doi.org/10.1046/j.1365-2699.2000.00489.x

Webb, N. J., & Tidemann, C. R. (1995). Hybridisation between black (*Pteropus alecto*) and grey-headed (*P. poliocephalus*) flying-foxes (Megachiroptera: Pteropodidae). *Australian Mammalogy*, *18*(1), 19–26. https://doi.org/10.1071/am95019

Webb, N. J., & Tidemann, C. R. (1996). Mobility of Australian flying-foxes, *Pteropus* spp. (Megachiroptera): Evidence from genetic variation. *Proceedings: Biological Sciences*, *263*(1369), 497–502. https://doi.org/10.1098/rspb.1996.0075

Welbergen, J. A., Meade, J., Field, H. E., Edson, D., McMichael, L., Shoo, L. P., Praszczalek, J., Smith, C., & Martin, J. M. (2020). Extreme mobility of the world's largest flying mammals creates key challenges for management and conservation. *BMC Biology*, *18*(1), 101. https://doi.org/10.1186/s12915-020-00829-w

Westcott, D. A., McKeown, A., Parry, H., Parsons, J., Jurdak, R., Kusy, B., Sommer, P., Zhao, K., Dobbie, M., Heersink, D., & Caley, P. (2015). Implementation of the national flying-fox monitoring program. Rural Industries Research and Development Corporation, Canberra.

Wiens, B. J., & Colella, J. P. (2024). triangulaR: An R package for identifying AIMs and building triangle plots using SNP data from hybrid zones. *bioRxiv*. https://doi.org/10.1101/2024.03.28.587167

Wiens, B. J., & Colella, J. P. (2025). That's not a hybrid: How to distinguish patterns of admixture and isolation by distance. *Molecular Ecology Resources*, *25*(3), e14039. https://doi.org/10.1111/1755-0998.14039

Wright, S. (1943). Isolation by Distance. *Genetics*, *28*(2), 114–138. https://doi.org/10.1093/genetics/28.2.114

Yi, X., & Latch, E. K. (2022). Nonrandom missing data can bias Principal Component Analysis inference of population genetic structure. *Molecular Ecology Resources*, *22*(2), 602–611. https://doi.org/10.1111/1755-0998.13498

Zhang, G., Cowled, C., Shi, Z., Huang, Z., Bishop-Lilly, K. A., Fang, X., Wynne, J. W., Xiong, Z., Baker, M. L., Zhao, W., Tachedjian, M., Zhu, Y., Zhou, P., Jiang, X., Ng, J., Yang, L., Wu, L., Xiao, J., Feng, Y., … Wang, J. (2013). Comparative analysis of bat genomes provides insight into the evolution of flight and immunity. *Science*, *339*(6118), 456–460. https://doi.org/10.1126/science.1230835

Zheng, X., Levine, D., Shen, J., Gogarten, S. M., Laurie, C., & Weir, B. S. (2012). A high-performance computing toolset for relatedness and principal component analysis of SNP data. *Bioinformatics*, *28*(24), 3326–3328. https://doi.org/10.1093/bioinformatics/bts606

Zhang, C., Nielsen, R. & Mirarab, S. (2025). CASTER: Direct species tree inference from whole-genome alignments. *Science*, 387(6737), eadk9688. https://doi.org/10.1126/science.adk9688